WSRC-MS-2002-00278

The Role of Al on the Thermodynamics of Hydrogen Absorption/Desorption by Some Ternary Pd-M-Al Alloys where M=Rh, Ni, Pt, Cr, Ag.

by
K. L. Shanahan
Westinghouse Savannah River Company
Savannah River Site
Aiken, South Carolina 29808

D. Wang
Chemistry Dept., University of Vermont
VT USA

T. B. Flanagan
Chemistry Dept., University of Vermont
VT USA

DOE Contract No. **DE-AC09-96SR18500**

This document was prepared in conjunction with work accomplished under Contract No. DE-AC09-96SR18500 with the U. S. Department of Energy.

DISCLAIMER

This report was prepared as an account of work sponsored by an agency of the United States Government. Neither the United States Government nor any agency thereof, nor any of their employees, makes any warranty, express or implied, or assumes any legal liability or responsibility for the accuracy, completeness, or usefulness of any information, apparatus, product or process disclosed, or represents that its use would not infringe privately owned rights. Reference herein to any specific commercial product, process or service by trade name, trademark, manufacturer, or otherwise does not necessarily constitute or imply its endorsement, recommendation, or favoring by the United States Government or any agency thereof. The views and opinions of authors expressed herein do not necessarily state or reflect those of the United States Government or any agency thereof.

This report has been reproduced directly from the best available copy.

Available for sale to the public, in paper, from: U.S. Department of Commerce, National Technical Information Service, 5285 Port Royal Road, Springfield, VA 22161,
phone: (800) 553-6847,
fax: (703) 605-6900
email: orders@ntis.fedworld.gov
online ordering: http://www.ntis.gov/support/index.html

Available electronically at http://www.osti.gov/bridge
Available for a processing fee to U.S. Department of Energy and its contractors, in paper, from: U.S. Department of Energy, Office of Scientific and Technical Information, P.O. Box 62, Oak Ridge, TN 37831-0062,
phone: (865)576-8401,
fax: (865)576-5728
email: reports@adonis.osti.gov

The Role of Al on the Thermodynamics of Hydrogen Absorption/Desorption by Some Ternary Pd-M-Al Alloys where M= Rh, Ni, Pt, Cr, Ag. (U)

D. Wang and Ted B. Flanagan
Chemistry Department, University of Vermont,
Burlington, VT 05405
and
Kirk L. Shanahan
Westinghouse Savannah River Company
Aiken, South Carolina 29802

Abstract

The solution of hydrogen and hydride formation in FCC substitutional solid solution $Pd_{0.9}Rh_{0.1-x}Al_x$ alloys have been examined. In contrast to some other Pd ternary alloys, a linear relation does *not* obtain between the H capacity and x for the $Pd_{0.9}Rh_{0.1-x}Al_x$ alloys investigated here where the H capacity of the alloys is estimated from the H content of the steeply rising part of the isotherms in the hydride phase regions. A linear increase of the dilute phase H solubility with x for these $Pd_{0.9}Rh_{0.1-x}Al_x$ alloys does, however, obtain for these alloys.

Although *Pd*-Rh binary alloys have broader plateaux than does Pd itself, small amounts of Al substituted into $Pd_{0.85}Rh_{0.15}$ or $Pd_{0.80}Rh_{0.20}$ alloys can reduce or eliminate the two phase regions, the plateaux; there is, however, not much effect on the dilute phase solubilities. For example, small amounts of Al substituted into the $Pd_{0.85}Rh_{0.15}$ or $Pd_{0.80}Rh_{0.20}$ alloys eliminate the plateaux. On the other hand, alloying Pd with Al to form binary alloys with X_{Al}=0.015 or 0.030 does not eliminate the plateaux which are present in these binary alloys up to X_{Al}=0.075 (298 K). Small amounts of Al substitution do not have such a dramatic effect on the plateau widths of the $Pd_{0.90}Ni_{0.10}$ and $Pd_{0.80}Ni_{0.20}$ alloys and similarly substitution of Al into *Pd*-Cr and *Pd*-Ag alloys does not introduce any anomalous effects into the isotherms.

Introduction

Pd alloys, like Pd itself, form hydride phases if the solute metal content is not too large. When the hydride phase forms by adding hydrogen to the dilute phase, the hydrogen pressure should be invariant at equilibrium because there are three phases and two components. This pressure, predicted to be invariant, is called the plateau pressure. The plateau pressures and H capacities are of the interest for possible applications of these systems. When the system is on the plateau the reaction which takes place upon H_2 (g) absorption is:

$$(1/2)H_2\ (g) + (1/(b+a))\ MH_a \rightarrow (1/(b+a))\ MH_b$$

where b and a are the H/M atom ratios of the co-existing hydride and dilute phases, respectively. Because of hysteresis, complete equilibrium is not attained and there is not a single plateau pressure but two, one for hydride formation and a lower one for decomposition.

The solution of hydrogen and hydride formation in binary solid solution Pd alloys have been examined for many different solutes [1, 2] and interest has now been extended to ternary Pd-rich alloys partly because of the possibility of obtaining desired properties of hydrogen absorption by variation in the amounts of two rather than just one solute as for the binary alloys.

The solution of hydrogen in binary *Pd*-Rh alloys has been studied by several workers [3-7]. These alloys are of interest because they, and possibly *Pd*—Ni alloys, are the only Pd alloys where the H capacity increases with solute metal concentration. This may be because Rh itself absorbs hydrogen to form a hydride phase at p_{H2} =3.8 GPa [8]. The absorption of hydrogen by *Pd*-Al alloys has been studied by Sakamoto *et al* [9] who found that the plateau pressures increase because these are contracted fcc lattices compared to Pd and the H capacities decrease with Al content such that there is no plateau for the $Pd_{0.90}Al_{0.10}$ alloy at 323 K [9]. The plateau pressures increase with % Al almost the same as with % Rh in the *Pd*-Rh system.

In this paper the effect of Al substitution on several Pd-rich alloys will be examined because it was observed in this laboratory that Al has a rather dramatic effect on the H capacity of several *Pd*-Rh alloys.

Experimental

The alloys were prepared by arc-melting the components under argon and then annealing them at 1133 K for 72 h. They were then rolled into thin foil and re-annealed at 1133 K for 24 h. In one series of experiments the compositions were chosen so that the Pd content was constant at X_{Pd}=0.90 and the total solute atom fraction, $X_{Rh} + X_{Al,}$ was kept at 0.10. For another series of experiments, small amounts of Al were added to *Pd*-Rh binary alloys such that they can be described as, e.g., $(Pd_{0.85}\ Rh_{0.15})_{0.985}Al_{0.015}$ which indicates that the $Pd_{0.85}\ Rh_{0.15}$ alloy is treated as one component of mol fraction 0.985 while Al is the other component with X_{Al}=0.015. If the composition were to be represented as atom fractions for this ternary alloy, the composition would be $Pd_{0.837}Rh_{0.148}Al_{0.0148}$ which is not as convenient as the other description.

Results and Discussion

$Pd_{0.9}Rh_{0.1-x}Al_x$ Alloys

Lattice Parameters

The lattice parameters for annealed $Pd_{0.9}Rh_{0.1-x}Al_x$ alloys were measured and the results are shown in Table 1. The parameters decrease with increase of x so that the alloys become more contracted as x increases and it would therefore be expected that ΔH_H^o and ΔH_{plat} for these "contracted" $Pd_{0.9}Rh_{0.1-x}Al_x$ alloys would decrease in magnitude with increase of x [1].

Table 1. Lattice Parameters of the $Pd_{0.9}Rh_{0.1-x}Al_x$ Alloys

$Pd_{0.90}Rh_{0.10}$	x=0.015	x=0.050	x=0.070	x=0.085	$Pd_{0.90}Al_{0.10}$
0.3882 nm	0.3880 nm	0.3877 nm	0.3876 nm	0.3877nm	0.3874 nm

where the parameter for the $Pd_{0.90}Al_{0.10}$ alloy is from reference 9.

Dilute Phase Hydrogen Solubilities.

The hydrogen solubilities as $H/M=r\rightarrow 0$ for annealed Pd and its alloys are described by Sieverts' law of ideal dilute solubility for a dissociating solute, $p^{1/2}=K_s r$. When solutes are substituted into Pd, the Sieverts' law constants, K_s, either decrease or increase depending upon whether the lattice expands or contracts, respectively, upon alloying. From the variation of the Sieverts'law constants with temperature, the standard relative enthalpies ΔH_H^o and entropies ΔS_H^o can be obtained where standard refers to infinite dilution of H. Sakamoto and coworkers [9-13] have obtained such thermodynamic values for several ternary alloy systems.

Figure 1 shows the dilute phase solubilities for $Pd_{0.9}Rh_{0.1-x}Al_x$ alloys from x=0 to 0.10 (323 K). The slopes increase steadily with decrease of x in passing from $Pd_{0.9}Al_{0.10}$ (x=0.1) to $Pd_{0.9}Rh_{0.10}$ (x=0). This is due mainly to the change of ΔH_H^o with x. The dashed curve in Figure 1 was calculated for the composition $Pd_{0.90}.Rh_{0.10}$ from the H_2 solubility in the $Pd_{0.9}Al_{0.10}$ alloy and the assumption that the only factor influencing the solubility is the enthalpy of solution in these two binary alloys; the values of ΔH_H^o for the two binary alloys were taken from the literature [6, 9]. The experimental error in these enthalpy data are enough to account for the deviation of the dashed line from the experimental solubility shown for the $Pd_{0.90}Rh_{0.10}$ alloy.

The Rh-rich alloys with x=0 and x=0.015 were quenched from the annealing temperature to room temperature in order to avoid phase separation during slow cooling [6]. It has been shown that the $Pd_{0.95}Rh_{0.05}$ alloy does not phase separate under these conditions [6]. Therefore, with the possible exception of the x=0.03 alloy, those with smaller Rh contents should not separate into two phases under these conditions.

A correlation can be made between log K_s, or equivalently , log $(p^{1/2}/atm^{1/2})$ at r=0.006, and x as shown in Figure 2. The correlation is quite linear except for the x=0.015 alloy which might have been on the line if a quenched alloy sample had been employed.

Some thermodynamic data were determined for the x=0.05 alloy in the dilute region using measured solubility relations from 303 K to 348 K (Fig. 3). Figure 4a shows a plot of $\Delta\mu_H/T$ against r and the intercepts give $\Delta\mu_H^o/T$ values which have been used in Figure 4b to obtain the thermodynamic parameters at infinite dilution of H. $\Delta\mu_H$ is the relative chemical potential of dissolved H, i.e., $\Delta\mu_H=\mu_H-½\,\mu_{H2}^o$, where the standard symbol on μ_{H2}^o refers to 1 bar and $\Delta\mu_H^o = \Delta H_H^o - T\,\Delta S_H^o$. From these slopes and intercepts, ΔH_H^o = -9.1 kJ/ mol H and ΔS_H^o = -58 J/ K mol H (Figs. 3, 4); the corresponding values for Pd-H are–10.2 kJ/ mol H and –55 J/ K mol H[14]. Hydrogen solution in the alloy is therefore not as exothermic as in Pd which is consistent with their greater plateau pressures.

Complete Hydrogen Isotherms.

An isotherm for the x=0.1 alloy has been measured at 323 K by Sakamoto *et al* [9] but because these results are rather crucial for the present research, an alloy was prepared in this laboratory and its isotherm measured at 323 K (Fig. 5). The agreement with the isotherm of Sakamoto *et al* is very good; there is no plateau or hysteresis for this alloy (323 K) although there is an inflection point in the isotherm indicative of supercritical behavior. Figure 5 also shows isotherms measured by Sakamoto et al [9] for the other *Pd*—Al alloys.

The complete hydrogen isotherms for different x values are shown in Figure 6 (323 K). The results are quite dramatic in that the H capacities and degrees of hysteresis both decrease markedly while the plateau pressures do not change very much. The average plateau pressure of the x=0 alloy and the region where there is an inflection point in the isotherm for the x=0.10 alloy are quite similar. All of the plateaux and the inflection region for the x=0.10 alloy are contained within the absorption and desorption plateau pressures for the x=0.015 alloy. Although substitutional Al and Rh affect the plateau pressures similarly, Al reduces the plateau breadth whereas Rh does not and, in fact, Rh is the only element, aside possibly from Ni, which increases the breadth. Although changes of the plateau pressures with x are insignificant, the hydrogen capacity and hysteresis change very significantly. Figure 7 shows these changes where it can be seen that neither the capacity nor hysteresis are linear functions of x. There is a sharp fall of the hysteresis, $RT \ln (p_d/p_f)^{1/2}$, at a composition of about x=0.02; p_f and p_d are the plateau pressures for hydride formation and decomposition. The H capacities are smaller in the region of Al atom fraction 0.03 than predicted by a linear relation between x=0 and 0.1 where the latter is taken as the position of the change of slope in the supercritical region. Teter and Thoma [15] have indicated that the H capacities of the $Pd_{0.9}Rh_{0.1-x}Co_x$ ternary alloys can be described in terms of a summation of the descriptions for the binary alloys. This is not the case for the present alloys.

Plateau thermodynamic parameters have been determined for the x=0.05 alloy from van't Hoff plots (Fig. 8) which give ΔH_{plat}= -15.8 and 16.8 kJ/ mol H and ΔS_{plat} = -49.8 and -52.6 J/ K mol H for absorption and desorption, respectively. The enthalpies are smaller in magnitude than those for Pd-H and the entropies are larger. These values are not as accurate as the dilute phase values because the hysteresis changes with temperature, i.e., there is hysteresis at 303 K but none at 348 K. The average plateau enthalpy of 16.3 kJ/ mol H is about the same as the calorimetric value for the $Pd_{0.90}Rh_{0.10}$ alloy [6] but larger than found for either the $Pd_{0.90}Al_{0.10}$ or $Pd_{0.95}Al_{0.05}$ alloys [9].

$(Pd_{0.85}\,Rh_{0.15})_{1-x}Al_x$ Alloys

The atom fractions of Al employed for the isotherm determinations of the $(Pd_{0.85}\,Rh_{0.15})_{1-x}Al_x$ alloys were 0.01, 0.02 and 0.03 on the basis of the corresponding total transition metal fractions, $X_{(Pd + Rh)}$, of 0.99, 0.98, 0.97. When these are converted into atom fraction of each component, the Al fraction is almost unchanged but the Pd and Rh atom fractions decrease, e.g., for the $(Pd_{0.85}\,Rh_{0.15})_{0.97}Al_{0.03}$ alloy they are 0.825 and 0.146, respectively. Results for the dilute phase of the $(Pd_{0.85}\,Rh_{0.15})_{1-x}Al_x$ alloys are shown in Figure 9 where there is seen to be very little difference in the dilute solubilities between the alloys including the binary $Pd_{0.85}\,Rh_{0.15}$ alloy. Since the changes in the Al content are small and it has been found for $Pd_{1-x}Al_x$ alloys that there is little change in the dilute solubilities from x=0 to about 0.050 [9], the result is not unreasonable.

Figure 10 shows complete isotherms (323 K) for the $(Pd_{0.85}\,Rh_{0.15})_{1-x}Al_x$ alloys where there is a dramatic decrease in the plateau breadths with increase of Al content. At only 3 at% Al, the plateau disappears and hysteresis vanishes. Isotherms for the binary *Pd*—Al alloys do not show such large changes in plateau breadths with Al content [9] as shown by the inset in Figure 10 where the variation of the plateau widths with X_{Al} are shown.

$(Pd_{0.80}\,Rh_{0.20})_{0.985}Al_{0.015}$

Figure 11 shows the effect of 1.5 at% Al on the plateau of the $Pd_{0.80}\,Rh_{0.20}$ alloy (273 K). The plateau has vanished even though the $Pd_{0.80}\,Rh_{0.20}$ alloy has a broader plateau than that of the $Pd_{0.85}\,Rh_{0.15}$ alloy which in turn has a broader one than Pd [6]. Although there is no plateau in this alloy, its single phase H_2 solubility is quite large, i.e., r≈0.6 at about 10 bar. Large single phase solubilities are desirable for certain applications such as for diffusion membranes where plastic deformation accompanying the abrupt hydride phase formation should be precluded.

From the results for the Al-substituted $Pd_{0.9}Rh_{0.1}$, $Pd0_{.85}\,Rh_{0.15}$, and $Pd_{0.80}\,Rh_{0.20}$ alloys, it can be concluded that the larger is the Rh content in the binary alloy, the greater is the effect of the substitutional Al on the breadth of the plateau even though the plateau breadth increases with X_{Rh} for these binary alloys.

$(Pd_{0.0.90}Ni_{0.10})_{0.985}Al_{0.015}$, $(Pd_{0.0.90}Ni_{0.10})_{0.970}Al_{0.030}$ and $(Pd_{0.0.85}Ni_{0.15})_{0.970}Al_{0.030}$, $(Pd_{0.0.80}Ni_{0.20})_{0.970}Al_{0.030}$ Alloys.

The alloys which are the most akin to the *Pd*-Rh alloys with respect to the plateau changes with X_{Ni} are the *Pd*-Ni alloys because Ni does not progressively decrease the breadth of the plateaux and both elements Rh and Ni form fcc hydride phases with H/M equal to nearly 1.0 but at high H_2 pressures. It is therefore of interest to examine the effect of small amounts of Al on the plateaux of some *Pd*-Ni alloys. Dilute phase hydrogen solubilities are shown for $(Pd_{0.90}Ni_{0.10})_{0.985}Al_{0.015}$ and $(Pd_{0.90}Ni_{0.10})_{0.970}Al_{0.030}$ alloys in Figure 12 where the Al is seen to cause a progressive decrease in H_2 solubilities. The complete isotherms for these two alloys are seen in Figure 13 where Al is seen to decrease the breadth of the plateaux but not as much as it does for the *Pd*—Rh alloys (Figs. 10, 11). Al increases the plateau pressure and shortens the plateau for the $(Pd_{0.0.85}Ni_{0.15})_{0.970}Al_{0.030}$ alloy but does not eliminate it or hysteresis (Fig. 14). When the Ni content increases to 0.20 as in the $(Pd_{0.0.80}Ni_{0.20})_{0.970}Al_{0.030}$ alloy, the effect of the Al is still not very dramatic (Fig. 15) as for the *Pd*-Rh alloys, e.g., the $(Pd_{0.80}\,Rh_{0.20})_{0.985}Al_{0.015}$ alloy where the plateau disappeared (Fig. 11). Thus the *Pd*-Ni alloys are not affected as much as the *Pd*-Rh alloys by small amounts of substitutional Al and the effect of Al does not increase with X_{Ni}.

***Pd*-Pt-Al Alloys.**

By contrast with the *Pd*-Ni and *Pd*-Rh binary alloys, substitution of Pt in Pd causes the plateaux to decrease in breadth rather sharply. Like Rh and Ni substitution, Pt increases the plateau pressures in binary Pd alloys [16]. Complete isotherms for the $(Pd_{0.95}Pt_{0.05})_{0.985}Al_{0.015}$ and $(Pd_{0.95}Pt_{0.05})_{0.970}Al_{0.03}$ alloys are shown in Figure 16 where there is a significant decrease in the H capacity but the plateaux are still present as is hysteresis. The greater amount of Al in the latter alloy causes a significantly greater decrease in the plateau widths. The dilute phase solubility is slightly greater for the former alloy. In the inset data for four cycles of the $(Pd_{0.95}Pt_{0.05})_{0.985}Al_{0.015}$ alloy are shown on an expanded scale and there is an anomalous looping in the third and fourth cycle isotherms as has been observed for *Pd*-Cr alloys [17].

The higher Pt content alloy $(Pd_{0.90}Pt_{0.10})_{0.975}Al_{0.025,}$ does *not* have a plateau and hysteresis has vanished (Fig. 17). There is a relatively large range of single phase hydrogen solubility which may be useful for an alloy where such a large range of H content is needed without the plastic work generated by hydride formation/decomposition.

$\mathbf{(Pd_{0.95}Cr_{0.05})_{0.975}Al_{0.025}}$ **Alloy.**

The isotherm for a $(Pd_{0.95}Cr_{0.05})_{0.975}Al_{0.025}$ alloy is shown in Figure 18 (323 K) where it can be seen that there is still a plateau and the effect of Al is the expected one of increasing the plateau pressures and slightly shortening the plateau. The increase of RT ln $p^{1/2}_f$ in passing from the $Pd_{0.95}Cr_{0.05}$ alloy to the $(Pd_{0.95}Cr_{0.05})_{0.975}Al_{0.025}$ alloy is 850 J/ mol H which is almost exactly the same as going from Pd to $Pd_{0.975}Al_{0.025}$.

$(Pd_{0.90}Ag_{0.10})_{0.970}Al_{0.03}$ Alloy.

All of the above binary Pd/M alloys can be classified as “contracted” alloys because their lattice parameters decrease with increase of substitutional M in Pd and consequently the plateau pressures all increase with increase of M. The substitution of Al increases the plateau pressures further. It was of interest to learn the effect of substitutional Al on the capacity of an “expanded alloy” that is, one whose unit cell is greater than Pd. The alloy chosen for this investigation was the $Pd_{0.90}Ag_{0.10}$ alloy which has a plateau pressure lower than for that for Pd since it is an expanded alloy. The $(Pd_{0.90}Ag_{0.10})_{0.970}Al_{0.03}$ alloy was prepared and this increased the plateau pressure relative to the binary alloy and decreased the plateau breadth (Fig. 19) similar to the changes which took place in the $(Pd_{0.90}Ni_{0.10})_{0.970}Al_{0.03}$ alloy (Fig. 13). There seems to be no difference between the contracted and expanded alloys with regard to their behavior with substitutional Al.

Predicted Effects of Al on the Plateaux of Some Pd—M Alloys Based on Linear Relationships between the Constituent Binary Alloys.

Table 2

Calculated and Experimental Values of P_f and (b-a) due to Al Substitution in *Pd*—M Alloys (323 K).

	P_f /bar (exp)	P_f /bar (calc)	(b-a) (exp)	(b-a) (calc)
$(Pd_{0.85}Rh_{0.15})_{0.980}Al_{0.02}$	4.7	7.5	0.20	0.39
$(Pd_{0.90}Ni_{0.10})_{0.970}Al_{0.03}$	3.2	3.7	0.23	0.31
$(Pd_{0.95}Pt_{0.05})_{0.970}Al_{0.03}$	0.64	0.68	0.23	0.31
$(Pd_{0.95}Cr_{0.05})_{0.975}Al_{0.025}$	1.2	1.1	0.25	0.27
$(Pd_{0.91}Ag_{0\cdot09})_{0.970}Al_{0.03}$	0.03	0.03	0.22	0.32

The change of log p_f with X_{Al} is linear for *Pd*-Al alloys (323 K) and therefore the value of p_f for any composition up to $X_{0.10}$ can be determined from this linear relation. If it is assumed that the ternary alloys’ values of log p_f change by the same amount with Al as the binary alloys, then the log p_f for the ternary alloys can be calculated from the following equation

$$\text{plateau } p_f(\text{binary Al})/p_f\,(\text{Pd}) = p_f(\text{ternary Al})/p_f\,(\text{binary})$$

where p_f(ternary Al) is the unknown. Some of the predicted plateau pressures are shown in Table 2 in comparison to the experimental values. The agreement is quite good except for the $(Pd_{0.85}Rh_{0.15})_{0.980}Al_{0.02}$ alloy.

Although log p_f is directly proportional to a thermodynamic quantity, ΔG_{plat} for the formation of the hydride phase, the plateau breadth is not directly proportional to a single thermodynamic parameter but is a more complex function of the thermodynamics of the system. The widths of the plateaux, (b-a), for the *Pd*-Al alloys are almost directly proportional to X_{Al} up to 0.10 where a and b are the lower and upper phase boundary compositions which are estimated from the isotherms. The plateau breadths are predicted by assuming that for the ternary alloys they are decreased by the same percentage as for the *Pd*-Al alloys. It can be seen from Table 1 that the agreement of the predicted with the experimental values is not very good indicating that the plateau breadth is reduced more by the substitution of Al to form binary alloys than it is reduced by the substitution of Al in pure Pd. The $(Pd_{0.80}Rh_{0.20})_{0.98}Al_{0.02}$ plateau breadth is reduced the most and $(Pd_{0.95}Cr_{0.05})_{0.975}Al_{0.025}$ the least, by Al substitution.

Possible Origin for the Large Effect of Al on the Plateaux of *Pd*—Rh Alloys.

Thermodynamics of Pd--H

The magnitudes of ΔH^o_H and ΔS^o_H do not affect the plateau breadth which is determined by *r*-dependent contributions to the H chemical potential. The *r*-dependent terms are the configurational entropy, the H-H interaction, and the influence of how band-filling by electrons donated from H influences the enthalpy of H_2 solution or, stated in a more general way, how the dissolved H affects the electronic structure of the alloy and how it, in turn, affects the enthalpy of H_2 solution. It seems necessary to first consider the thermodynamic origins of two phase formation in Pd-H and then in *Pd*-Rh-H alloys.

Figure 20a shows the various contributions to $\Delta\mu_H = \mu_H - ½\, \mu_{H2}^o$ as a function of *r* for the Pd-H system at 300 K where the necessary data were taken from reference [14]; for convenience in this plot $\Delta\mu_H^o$ is taken as zero which does not affect the two phase boundaries. The equation for ΔG_{plat} is

$$RT\ln p^{1/2}_{plat} = \Delta G_{plat} = \Delta\mu_H^o + [RT/(b-a)]\,[b \ln b - a \ln a + (1-b)\ln (1-b) - (1-a)\ln (1-a)] + \Delta\mu^E_{plat} \quad (1)$$

where $\Delta\mu^E_{plat} = (b-a)^{-1}\int_a^b \mu_H^E(r)dr$, $\Delta\mu_H^o = \mu_H^o - (1/2)\,\mu_{H2}^o$ and μ_H^o is the value at infinite dilution of H [17]. The presence of two solid phases is shown by the loops in the $\Delta\mu_H$–*r* relation where the rule of equal areas can be employed to determine the plateau pressure and phase boundary compositions. The value of ΔH_{plat} is determined by the position of the horizontal line which satisfies: $(b-a)\Delta H_{plat} = \int_a^b \Delta H_H dr$ as shown in Figure 20b where a value of -22 kJ/ mol H is obtained for ΔH_{plat} by this method which is somewhat too large since the calorimetric value at 300 K is –19.2 kJ/ mol H [18] and the discrepancy must be due to some errors in the data of [14].

Thermodynamics of Pd-Rh-H

μ_H^E is determined by the non-ideal configurational entropy and other H-dependent contributions to the entropy and enthalpy. Rh, like Pd, forms an almost stoichiometric RhH hydride within the fcc metal, although P_{H2} =38 GPa is needed to form Rh hydride. The high P_{H2} needed for Rh is mainly due to the $|\Delta H_H^o|$ term. The H-dependent terms such as the configurational entropy and the H—H interactions might be expected to be qualitatively rather similar for Pd and the *Pd*- Rh alloys since their plateau breadths are similar. There is experimental evidence that their $|\Delta H_H|$-*r* relations have similar shape for the alloys as for Pd [6,18] because the $|\Delta H_H|$ values both increase as *r* increases from 0 and decrease with *r* in the hydride phase. The $|\Delta H_H(r)|$ relationships for the *Pd*-Rh alloys must be consistent with the measured values of $|\Delta H_{plat}|$ which are smaller than those for Pd-H and decrease with X_{Rh} and also the plateaux are somewhat broader than for Pd-H. These two requirements mean that the $|\Delta H_H(r)|$ against *r* relation must be somewhat flatter with smaller $|\Delta H_H(r)|$ values than for Pd-H, a tendency which must increase with X_{Rh}. Experimentally the difference between $|\Delta H_{plat}|$ and $|\Delta H_H^o|$ decreases with X_{Rh} [6] and, in fact this may be characteristic of all Pd alloys because the solvus compositions always increase relative to Pd-H [1]. With reference to Figure 20b, this difference for Pd-H is represented by the distance between the horizontal dashed line indicating $|\Delta H_{plat}|$ and $|\Delta H_H|$=10.2 kJ/ mol H; for the *Pd*-Rh alloys this distance becomes progressively smaller with increase of X_{Rh}. The smaller differences for the alloys require that the $|\Delta H_H(r)|$ relations are flattened as X_{Rh} increases compared with Pd-H.

$\Delta\mu^E_{plat} = \Delta G_{plat} - \Delta^o\mu_H$ – [ideal configurational term], is almost equal for Pd and all the *Pd*-Rh alloys which is consistent with the expectation that the H-dependent terms in μ_H be similar for Pd and Rh. Figure 21 shows a plot of ΔG_{plat} plotted against $\Delta^o\mu_H$ and the intercept is equal to $\Delta\mu^E_{plat}$ + (ideal configuration term). Such a plot is not linear for Pd alloys where the plateau widths decrease markedly with M which includes most Pd binary alloys. The corresponding values of ΔS_{plat}^E and ΔH_{plat}^E were determined (Table 3) and there are compensating changes of $-T\Delta S_{plat}^E$ and ΔH_{plat}^E with X_{Rh} which keeps $\Delta\mu^E_{plat}$ constant. The values of $-T\Delta S_{plat}^E = -T(b-a)^{-1}\int_a^b S_H^E(r)dr$ decrease with X_{Rh} while ΔH_{plat}^E increases. The calculation of these excess plateau values depends on the values of ΔH_H^o and ΔS_H^o which were determined elsewhere earlier [6]. The values of ΔS_H^o appear to be somewhat anomalous because they become increasingly negative with X_{Rh} (Table 3) and, for this reason, values for a typical alloy, X_{Rh}=0.20, were redetermined in this work. The results (Table 3) are in good agreement with the earlier data. It is difficult to explain large negative values because they normally indicate that some interstices are excluded from occupation as for *Pd*-Ag alloys where H apparently avoids Ag nearest neighbors [19]; it seems unlikely for H to avoid Rh nearest neighbors in *Pd*-Rh alloys because such excluded interstices in the dilute phase must be occupied in the hydride phase because of the large H contents. Another possibility for large negative ΔS_H^o values are an increase in the contribution of S^{el}_H [20] to the entropy because the electronic heat capacity should of the alloys should increase with X_{Rh}. The heat capacities of *Pd*-Rh alloys increase with Pd [21] and therefore if H also acts to donate electrons to the d-band of Rh, in the same way as Pd, then the partial electronic entropy due to H should be positive and this could cause ΔS_{plat}^E to increase with X_{Rh}.

Table 3. Thermodynamic Properties of *Pd*/Rh Alloys from reference 6 and the last three Columns were Calculated here from the Earlier Data. Enthalpies and free energies are in kJ/ mol H and entropies are in J/K mol H.

X_{Rh}	ΔG_{plat}	ΔH_{plat}	ΔS_{plat}	$\Delta\mu^o_H$	$\Delta H_H{}^o$	$\Delta S_H{}^o$	$\Delta G^E{}_{plat}$	$\Delta H^E{}_{plat}$	$\Delta S^E{}_{plat}$
0	-4.3	-19.5	-46.0	7.2	-10.2	-54.0	-9.3	-9.3	-0.8
0.05	-2.3	-17.7	-47.8	9.1	- 9.1	-56.5	-8.9	-8.6	0.9
0.10	0.12	-16.1	-49.1	11.0	-8.5	-60.3	-9.3	-7.6	4.0
0.15	1.75	-14.2	-49.4	12.6	-7.9	-63.4	-9.6	-6.3	7.2
0.20	3.42	-12.8	-50.3	14.0	-7.3(-7.5)	-66.0(-66.3)	-9.6	-5.5	10.9
0.25	5.00	-11.2	-50.0	15.6	-6.6	-68.7	-9.5	-4.6	14.5

The values in parenthesis have been determined in this research and $\Delta\mu^o{}_H$ and $\Delta S_H{}^o$ have been evaluated assuming that all of the interstices are available for occupation.

Thermodynamics of Pd-Rh-Al-H

It is difficult to understand why Al reduces the plateau widths of the *Pd*-Rh alloys so dramatically and why the effect increases with X_{Rh}. Substitutional Al in *Pd*-Rh alloys must alter the electronic structure rather markedly because, for example, although the plateau of a $Pd_{0.80}Rh_{0.20}$ alloy is wider than for Pd itself [6], it disappears in the $(Pd_{0.85}Rh_{0.15})_{0.970}Al_{0.03}$ and $(Pd_{0.80}Rh_{0.20})_{0.985}Al_{0.015}$ alloys (Figs. 10, 11) where the fractions of Al are quite small. $\Delta\mu^E{}_{plat}$ does not stay nearly constant with Al content for $Pd_{0.90}Rh_{(0.1-x)}Al_x$ alloys as it does for the *Pd*-Rh alloys. The amounts of Al in these alloys are too small to significantly affect the fraction of available interstices and therefore the effect must be related to non-configurational entropy. By contrast, larger amounts of Al do not lead to plateau disappearance in Pd or the $Pd_{0.90}Rh_{0.10}$ alloy.

Al donates 3 electrons to the d-band of Pd judging from magnetic susceptibility changes of *Pd*-Al alloys [22]. On the basis of this research, Al greatly suppresses two phase formation in alloys where the solutes also have holes in their d-bands such as *Pd*-Rh but the effect of Al on the plateaux of alloys such as *Pd*-Ag or Pd itself, it not unusual. It seems that the origin of the effect is in the changing of the electronic structure of the alloys but the details are not known at present.

Conclusions

The capacities of most of the Al-containing ternary alloys are smaller than predicted from the effect of Al on the capacities in binary *Pd*-Al alloys and the capacity of a *Pd*-Rh alloy is most decreased by Al. The plateau pressures are reasonably well predicted by the changes of p_f with Al in the binary *Pd*-Al alloys. The most striking results are for the $(Pd_{0.85}Rh_{0.15})_{0.97}Al_{0.03}$ and $(Pd_{0.80}Rh_{0.20})_{0.97}Al_{0.03}$ alloys. It would be of interest to measure the electronic heat capacities of these alloys where the plateau has disappeared.

Acknowledgements

The authors wish to thank J. D. Clewley for help in sample preparation, etc.

References

1. Y. Sakamoto, K. Ohira, F. Chen, M. Ura, T. Flanagan, *Ber. Bunsenges Phys. Chem.*, **99** (1995) 807.
2. A. Weiss, S. Ramaprabhu, N. Rajalakshmi, *Zeit. Physik. Chem*., **199** (1997) 165.
3. B. Baranowski, S. Majchrzak, T. Flanagan, *J. Physical Chem.*, **77** (1973) 35.
4. T. Witherspoon, W. Mcfall, F. Lewis, *Nature*, **44** (1973) 2442.
5. J. Clewley, J. Lynch, T. Flanagan, *J.Chem. Soc., Faraday Trans. I*,**73** (1977) 494.
6. H. Noh, W. Luo, T. Flanagan, *J. Alloys Compounds*, **196** (1993) 7.
7. Y. Sakamoto, Y. Haraguchi, M. Ura, F. Chen, *J. Alloys Compounds*, **98** (1994) 964.
8. M. Tkacz, *J. Chem. Phys.*, **108,** (1998) 2084.
9. Y. Sakamoto, E. Kakhisa, Y. Kinari, Z*eit. Physik. Chem.*, **179** (1993) 69.
10. Y. Sakamoto, N. Ishimaru, Y. Inoue, *Ber. Bunsenges Physik. Chem.*, **96** (1992) 128.
11. Y. . Sakamoto, N. Ishimaru, Y. Mukai, *Ber. Bunsenges Physik. Chem.*, **95** (1991) 680.
12. Y. Sakamoto, K. Ohira, M. Kokubu, T. Flanagan, *J. Alloys Compounds*, **253-254** (1997) 212.
13. Y. Sakamoto, K. Ohira, N. Ishimaru, F. Chen, M. Kokubu, T. Flanagan, *J. Alloys Compounds*, **217** (1995) 226.
14. T. Kuji, W. Oates, B. Bowerman, T. Flanagan, *J. Phys. F:Met. Phys.*, **13** (1983) 1785.
15. D. Teter, D. Thoma, *Met. Mater. Trans. B*, **30B**, (2000) 667.
16. H. Noh, T. Flanagan, T. Sonoda, Y. Sakamoto, *J. Alloys Compounds*, **228** (1995) 164.
17. D. Wang, J. Clewley, S. Luo, T. Flanagan, *J. Alloys Compounds*, **325** (2001) 151
18. T. Flanagan, W. Luo, J. Clewley, *J. Less-Common Mets.*, **172-174** (1991) 42.
19. T. Flanagan, W. Oates, *Ann. Rev. Mater. Sci.*, **21** (1991) 269.
20. W. Oates, T. Flanagan, *Solid State Comm*., **9** (1971) 1841
21. F. Hoare, in *Electronic Structure and Alloy Chemistry of the Transition Metals*, ed. P. Beck, Interscience Pub., New York, 1963.
22. M. Glugla, H. Severin, G. Sicking, *Phys. Status Solidi*, **106** (1981) 505.

Figure Captions

Figure 1. Dilute phase H_2 solubilities in Pd $_{0.90}Rh_{0.1-x}Al_x$ (323 K). Solid curve without points, Pd; ○, $Pd_{0.90}Al_{0.10}$; •, $Pd_{0.90}Rh_{0.015}Al_{0.085}$; Δ, $Pd_{0.90}Rh_{0.03}Al_{0.07}$; ▲, $Pd_{0.90}Rh_{0.05}Al_{0.05}$; ∇, $Pd_{0.90}Rh_{0.07}Al_{0.03}$; ▼, $Pd_{0.90}Rh_{0.085}Al_{0.015}$; □, $Pd_{0.90}Rh_{0.10}$.

Figure 2. Dilute phase solubilities (323 K) as indicated by log $p^{1/2}$ at r=0.006 as a function of x.

Figure 3. Dilute phase solubilities of the Pd $_{0.90}Rh_{0.05}Al_{0.05}$ alloy at: Δ, 303 K, ○, 323 and ∇, 348 K.

Figure 4. (a) Plots of $(\Delta\mu_H)/RT$ (=ln $p^{½}(1-r)/r$ against r at several temperatures for the $Pd_{0.90}Rh_{0.05}Al_{0.05}$ alloy. (b) Plots of the intercepts at $r=0$, $\Delta\mu^o{}_H/T$, of the plots shown in (a) as a function of 1/T.

Figure 5. An isotherm for the x=0.10 alloy ($Pd_{0.90}Al_{0.10}$) along with isotherms at 323 K for other *Pd*—Al alloys from reference 9. ○, present absorption data; •, present desorption data; Δ, from reference 9.

Figure 6. Complete isotherms (323 K) for the Pd $_{0.90}Rh_{0.1-x}Al_x$ alloys. Open symbols are for absorption and filled symbols for desorption. The numbers on the curves indicate atom fraction Al.

Figure 7. Plots of the degree of hysteresis and β_{min} which is the r value at the upper end of the plateau for the Pd $_{0.90}Rh_{0.1-x}Al_x$ alloys (323 K) as estimated from Figure 6.

Figure 8. Van't Hoff plots for the plateau pressures evaluated at r =0.20 for the Pd $_{0.90}Rh_{0.05}Al_{0.05}$ alloy. ○, absorption data; •, desorption data.

Figure 9. Dilute phase solubilities for $(Pd_{0.85}Rh_{0.15})_{(1-x)}Al_x$ alloys (323 K). ○, for x=0; Δ, x=0.01; ∇, x=0.02; □ , x=0.03.

Figure 10. Complete isotherms for the $(Pd_{0.85}Rh_{0.15})_{(1-x)/}Al_x$ alloys (323 K). ○, x=0; Δ, x=0.01; ∇, x=0.02; □, x=0.03. The open symbols for absorption and filled ones for desorption. The inset shows the extent of the plateaux for these alloys and the *Pd*-Al alloys. ○, Pd-Al alloys. Δ, $(Pd_{0.85}Rh_{0.15})_{(1-x)}Al_x$ alloys.

Figure 11. Isotherm for the $(Pd_{0.80}Rh_{0.20})_{0.985}Al_{0.015}$ alloy compared to the $Pd_{0.80}Rh_{0.20}$ alloy (273 K). Δ, annealed $Pd_{0.80}Rh_{0.20}$ alloy; o, $(Pd_{0.80}Rh_{0.20})_{0.985}Al_{0.015}$ alloy. Open symbols are for absorption and filled ones for desorption.

Figure 12. Dilute phase data (323 K) for $Pd_{0.90}Ni_{0.10}$ and $(Pd_{0.90}Ni_{0.10})_{1-x}Al_x$ alloys. □, $Pd_{0.90}Ni_{0.10}$; Δ, $(Pd_{0.90}Ni_{0.10})_{0.985}Al_{.015}$ alloy; o, $(Pd_{0.90}Ni_{0.10})_{0.97}Al_{0.030}$ alloy.

Figure 13. Complete isotherms (323 K) for the $Pd_{0.90}Ni_{0.10}$ and $(Pd_{0.90}Ni_{0.10})_{1-x}Al_x$ alloys. ---, $Pd_{0.90}Ni_{0.10;}$ o, $(Pd_{0.90}Ni_{0.10})_{0.985}Al_{.015}$ alloy; Δ, $(Pd_{0.90}Ni_{0.10})_{0.97}Al_{0.030}$ alloy. Open symbols are for absorption and filled ones for desorption.

Figure 14. Complete isotherms (323 K) for the $Pd_{0.85}Ni_{0.15}$, Δ, and $Pd_{0.85}Ni_{0.15})_{0.97}Al_{0.015,}$ o, alloys. Open symbols are for absorption and filled ones for desorption.

Figure 15. Complete isotherms (323 K) for the $Pd_{0.80}Ni_{0.20}$, ----, $(Pd_{0.80}Ni_{0.20})_{0.97}Al_{0.03\,,}$ o , alloys. Open symbols are for absorption and filled ones for desorption.

Figure 16. Complete isotherms (323 K) for the $Pd_{0.80}Pt_{0.05}$ and $(Pd_{0.95}Pt_{0.05})_{1-x}Al_x$ alloys. ---, $Pd_{0.95}Pt_{0.05;}$ Δ, $(Pd_{0.95}Pt_{0.05})_{0.985}Al_{0.015}$ alloy (1st cycle); □, $(Pd_{0.95}Pt_{0.05})_{0.97}Al_{0.030}$ alloy. The insert shows more detailed behavior with anomalous isotherm behavior, i.e., "van der Waal"-like loops, for the $(Pd_{0.95}Pt_{0.05})_{0.985}Al_{0.015}$ alloy. Δ, 1st cycle, ∇, 2nd cycle, □, 3rd cycle, x, 4th cycle. Open symbols are for absorption and filled ones for desorption.

Figure 17. Complete isotherms (323 K) for $Pd_{0.90}Pt_{0.10}$ and the $(Pd_{0.90}Pt_{0.10})_{0.975}Al_{0.025}$ alloys. Δ, $Pd_{0.90}Pt_{0.10;}$ o, $(Pd_{0.90}Pt_{0.10})_{0.975}Al_{0.025}$.

Figure 18. Complete isotherms (323 K) for the $Pd_{0.95}Cr_{0.05}$, Δ, and $(Pd_{0.95}Cr_{0.05})_{0.975}Al_{0.025}$, o ,alloys. Open symbols are for absorption and filled ones for desorption.

Figure 19. Complete isotherms (323 K) for the $Pd_{0.91}Ag_{0.09}$, Δ, and the $(Pd_{0.91}Ag_{0.09})_{0.97}Al_{0.03}$, o, alloys. .

Figure 20. Upper figure, plots of the various contributions to μ_H for Pd—H (300 K) using data from reference 14. The value of μ_H^o is assumed to be 0 for convenience, μ_H^E is the excess chemical potential of H due to non-ideal terms and $\mu_H^{id,\,config}$ is the ideal configurational chemical potential. The sum of the various curves has loops as shown and the rule of equal areas locates the co-existing phase boundaries and plateau pressure. The lower figure is a plot of ΔH_H as a function of *r* [14]. ΔH_{plat} is located by the equivalence of the areas from *a* to *b* of the continuous plot and the rectangular area (*b*-*a*)ΔH_{plat} .

Figure 21. Plot of $\Delta^o\mu_H$ against ΔG_{plat} for *Pd*-Rh alloys (323 K).

Figure 1.

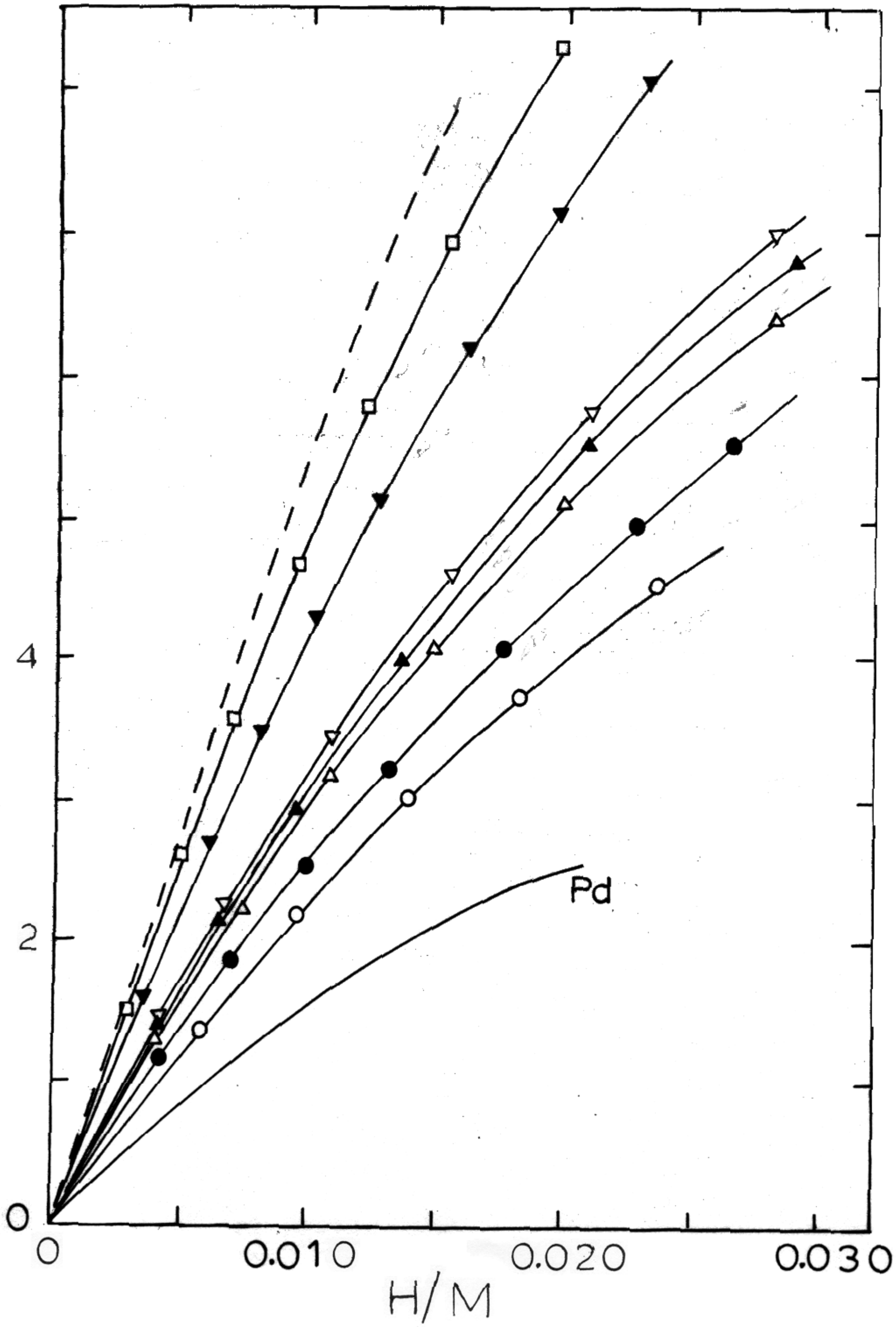

Figure 2.

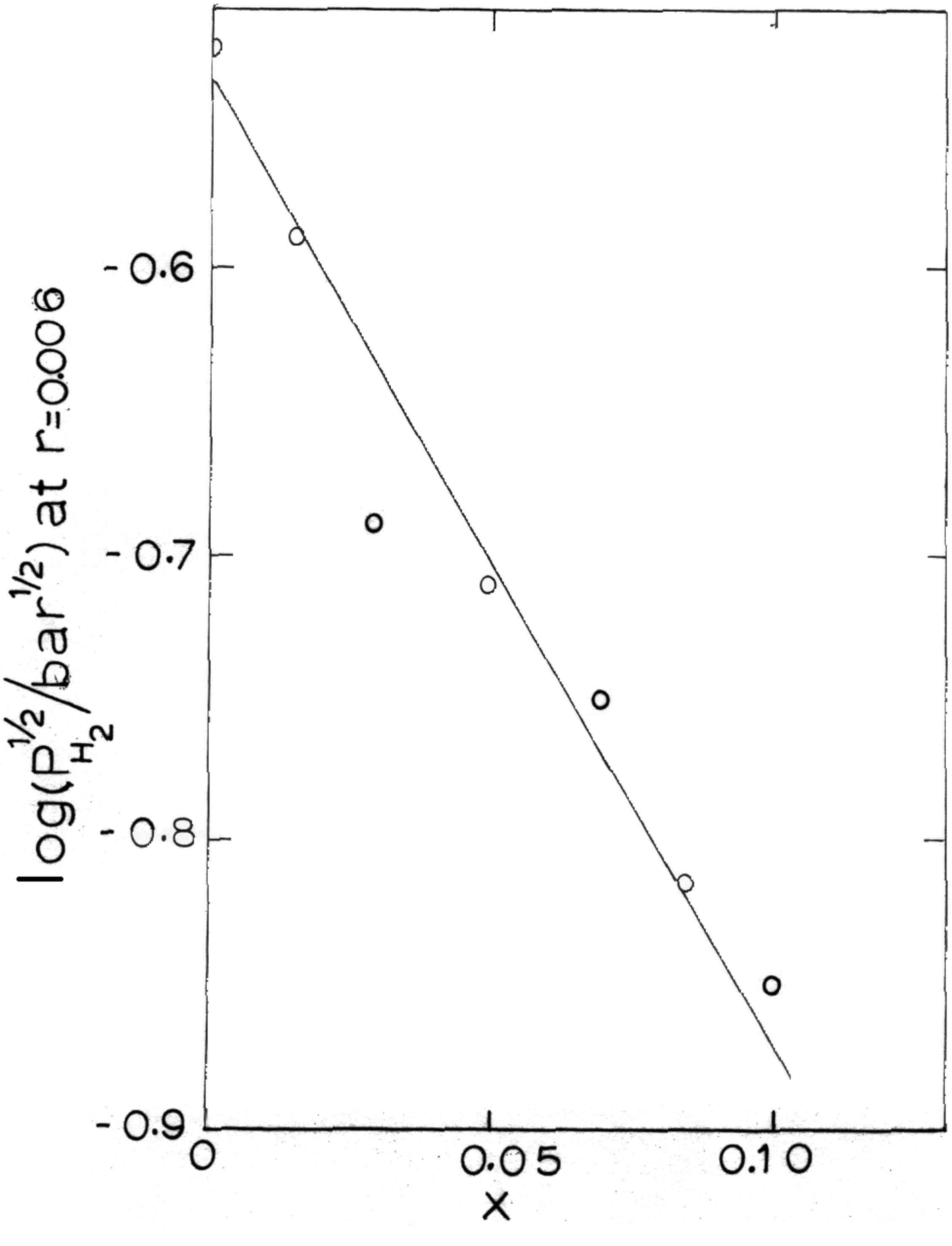

Figure 3.

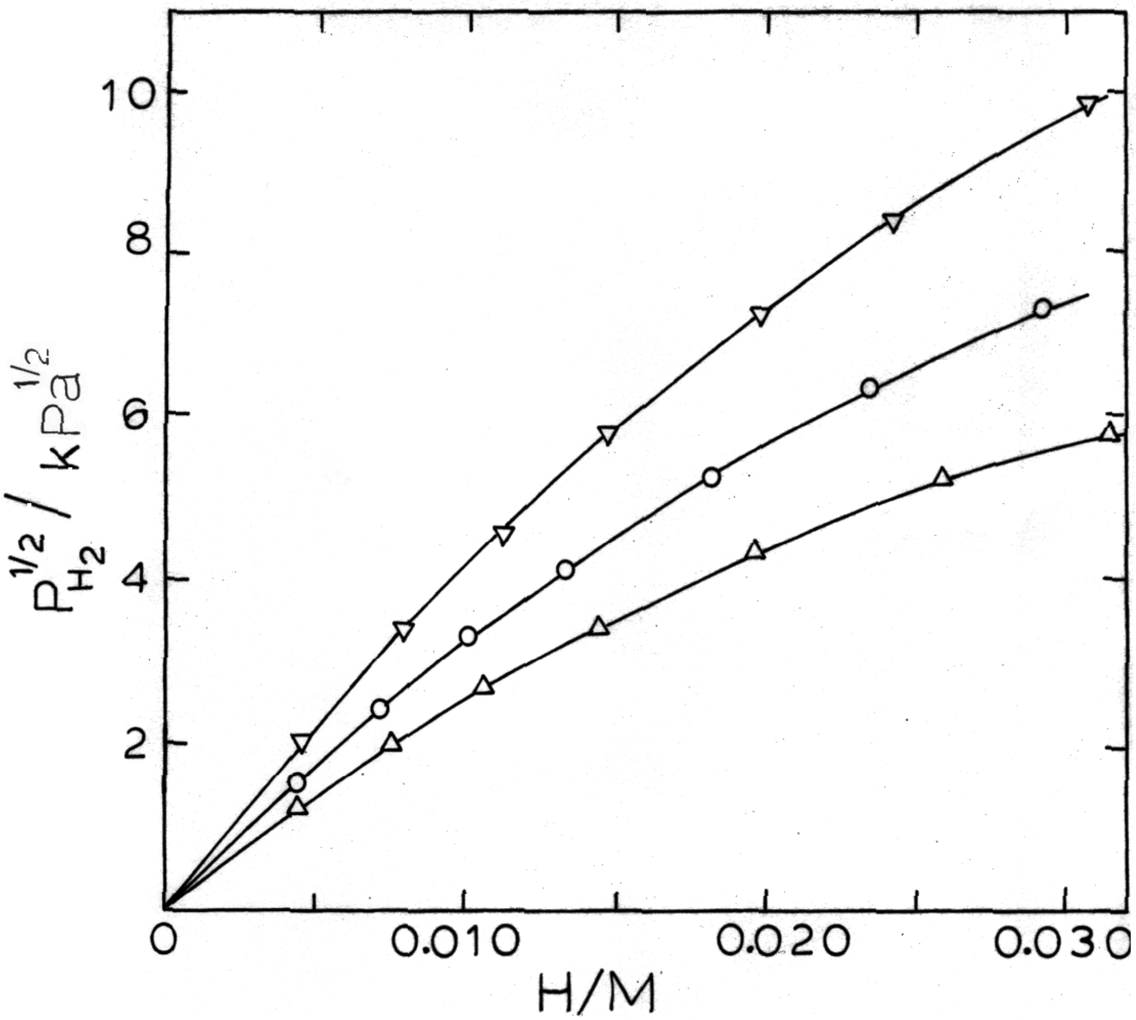

Figure 4.

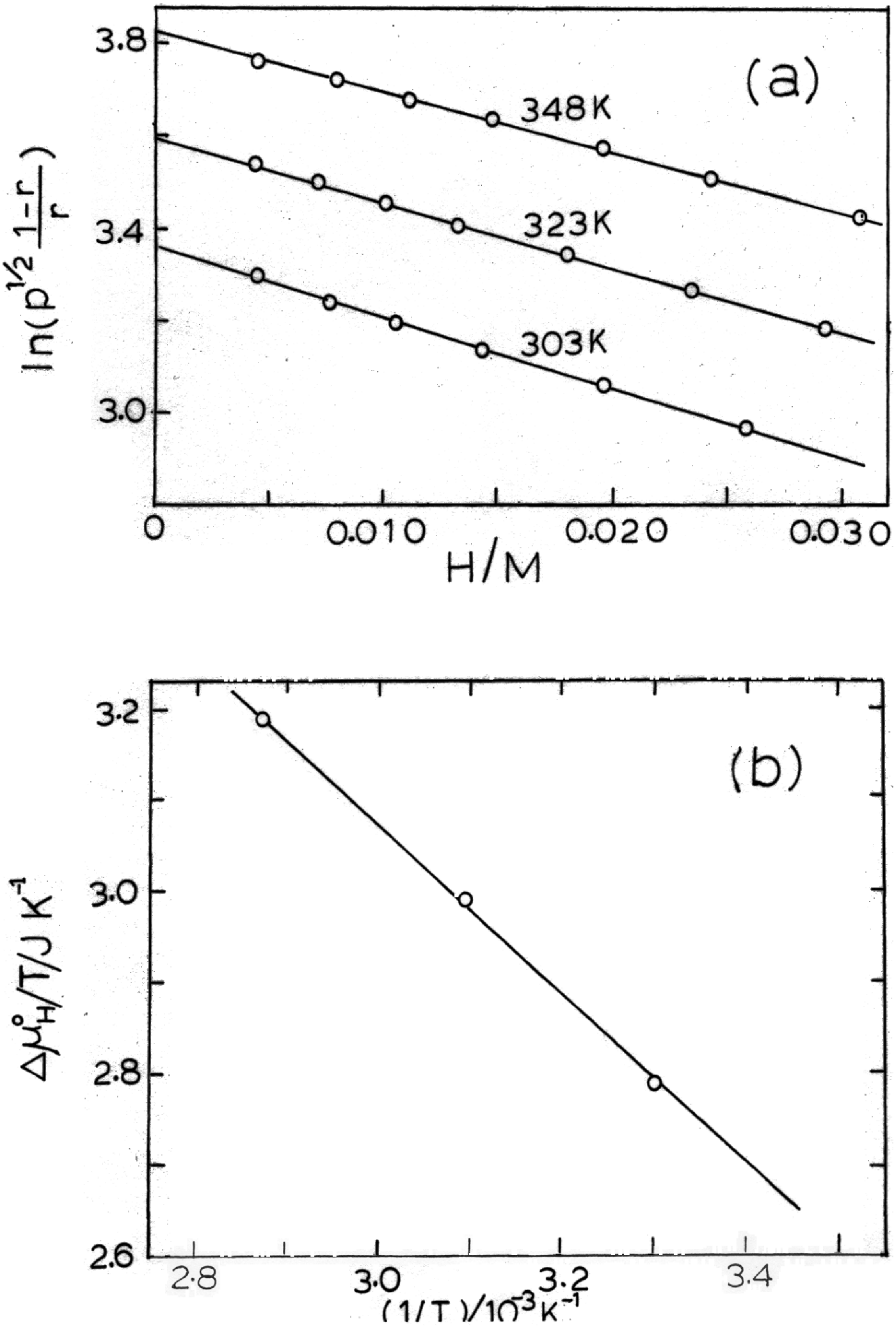
(a)
ln(p^½ (1-r)/r)
3.8
3.4
3.0
348K
323K
303K
0
0.010
0.020
0.030
H/M
(b)
Δμ°H/T/J K⁻¹
3.2
3.0
2.8
2.6
2.8
3.0
3.2
3.4
(1/T)/10⁻³K⁻¹

Figure 5.

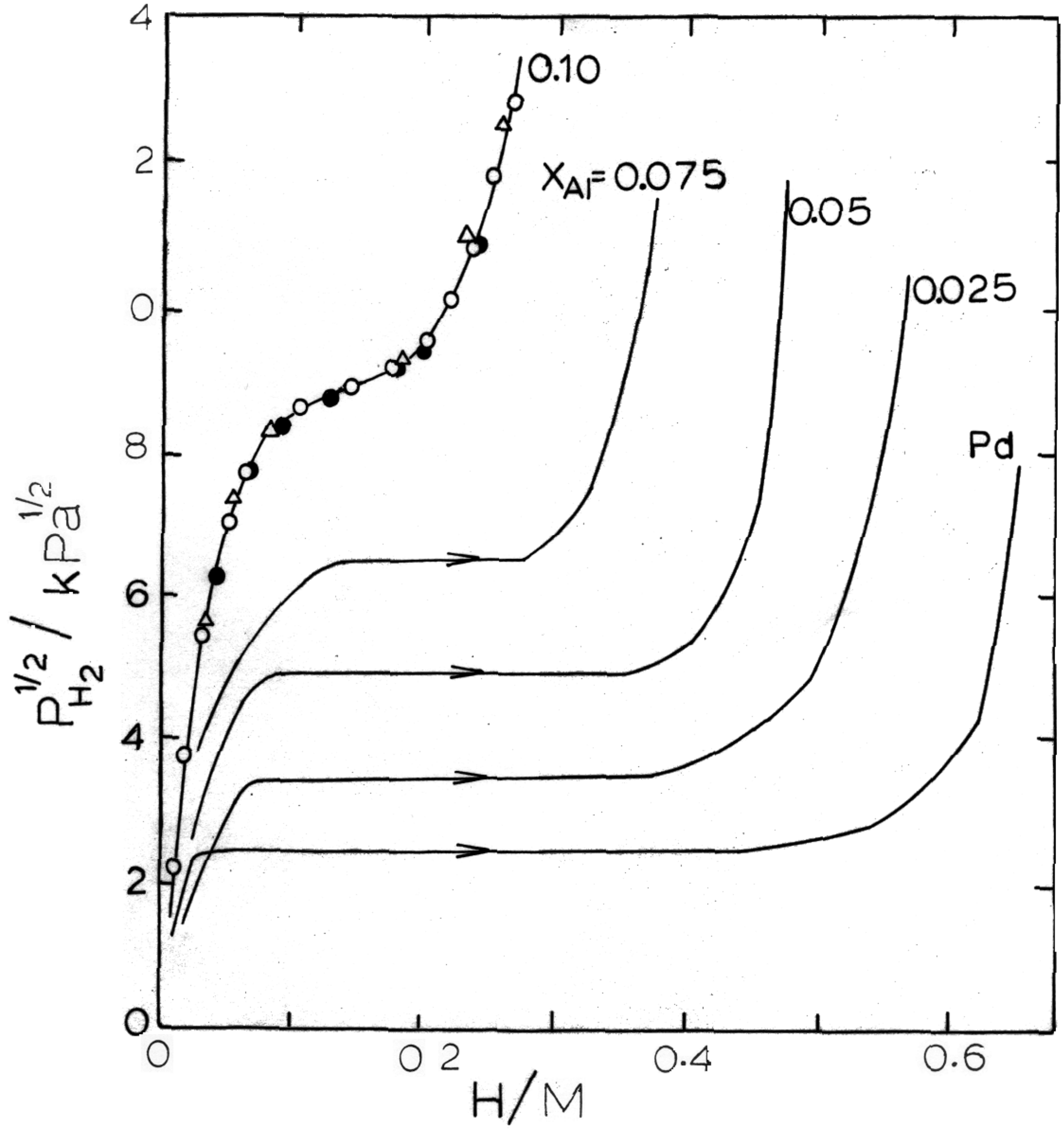

Figure 6.

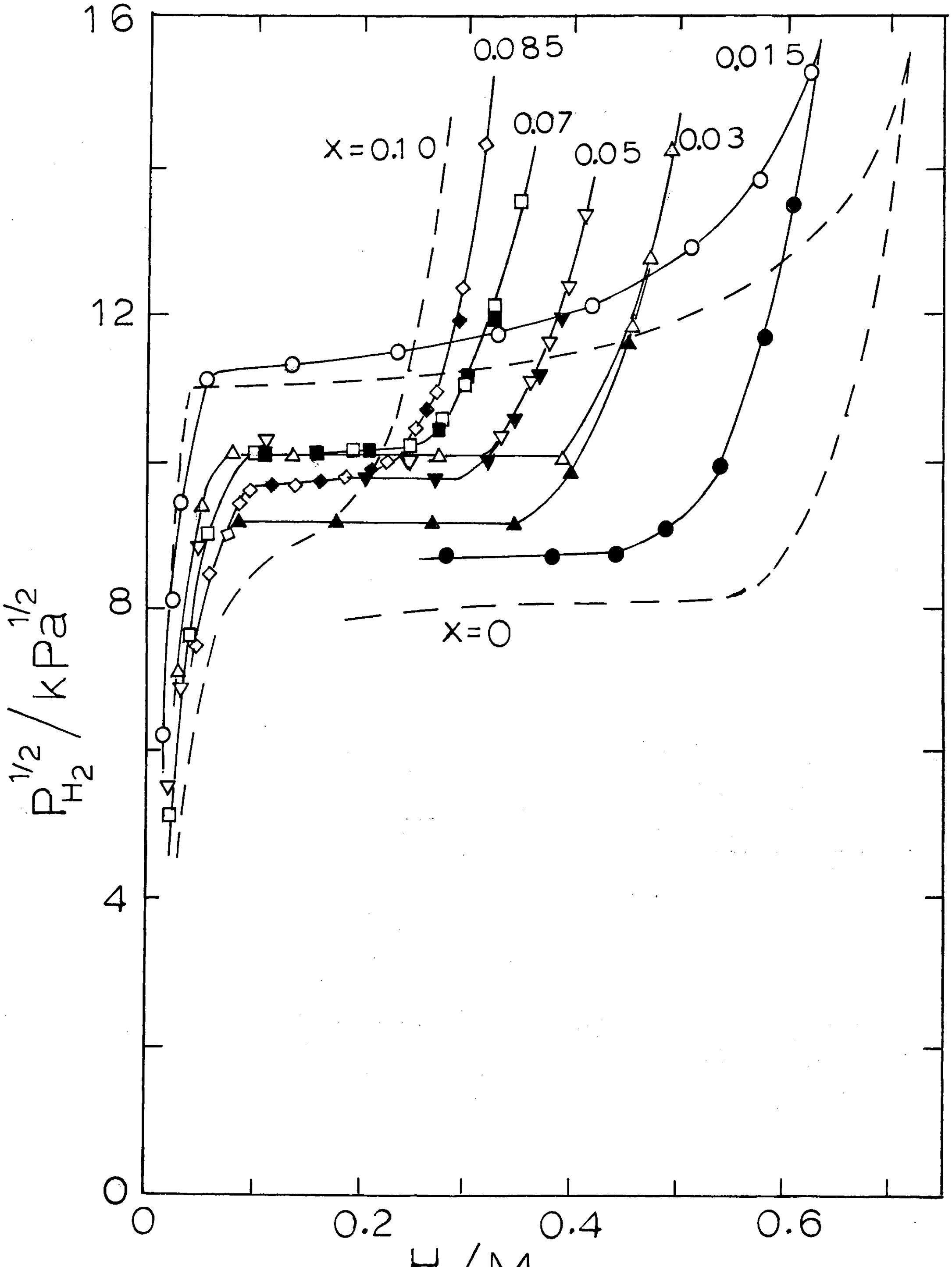

Figure 7.

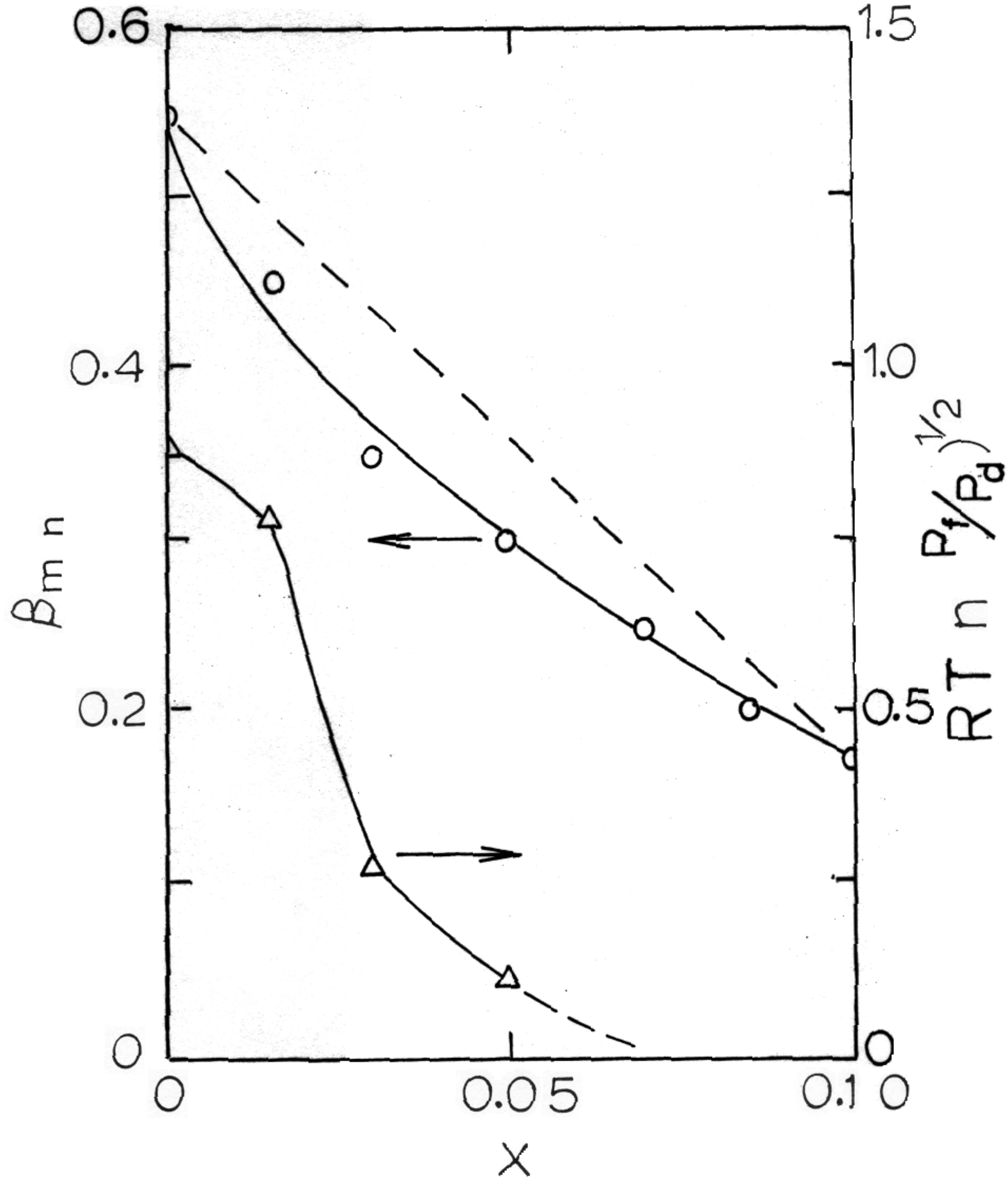

Figure 8.

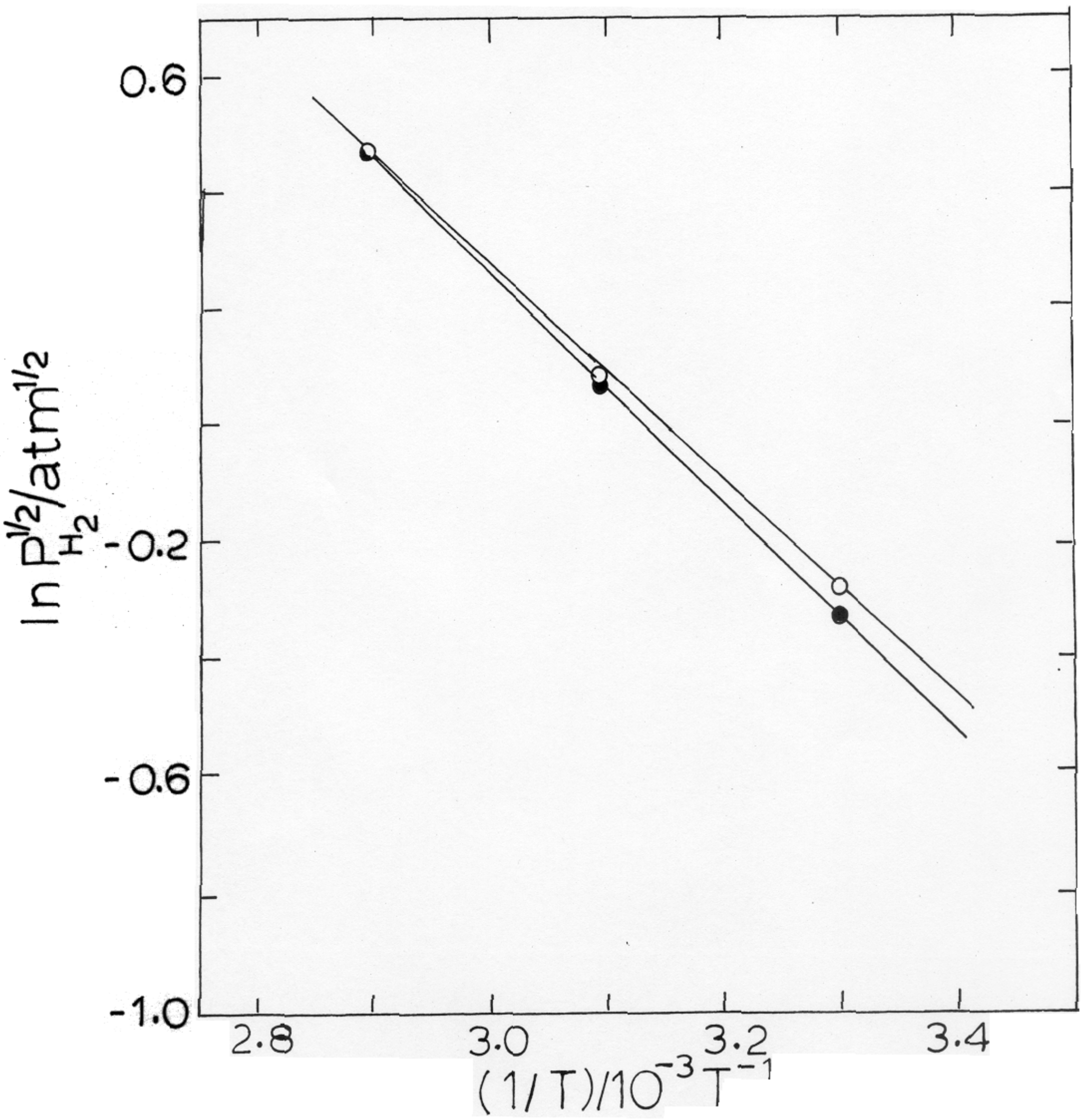

Figure 9.

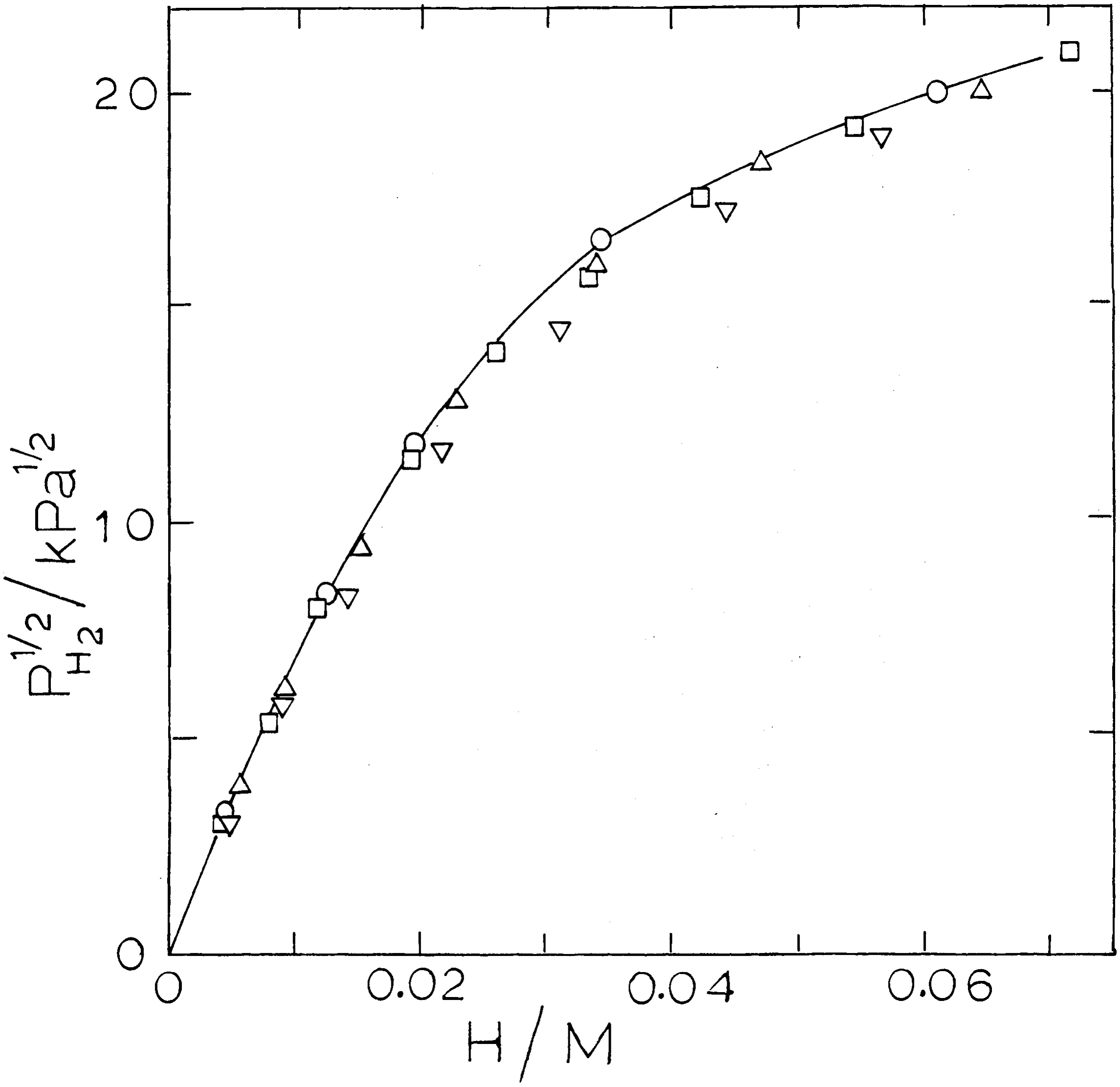

Figure 10.

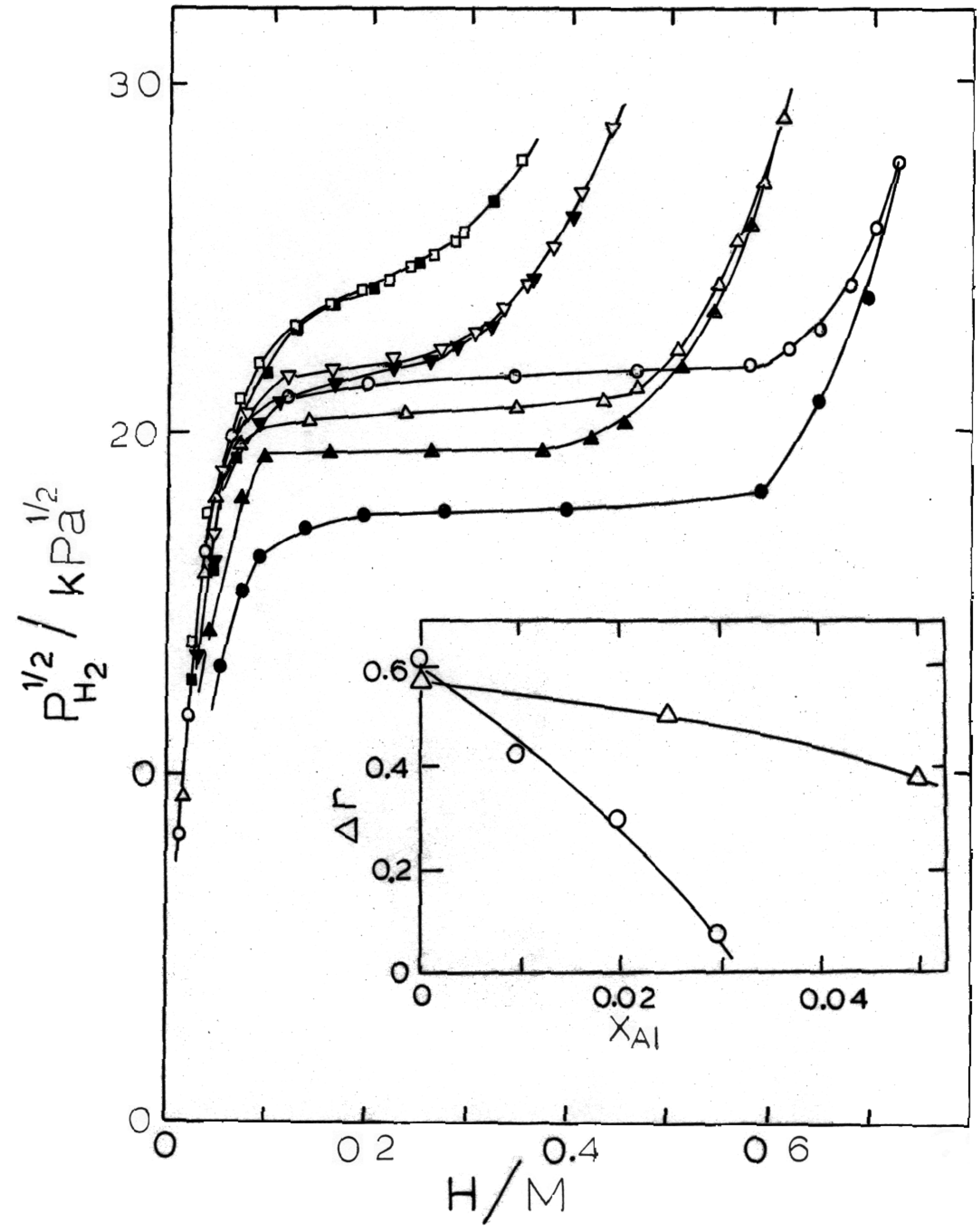

Figure 11.

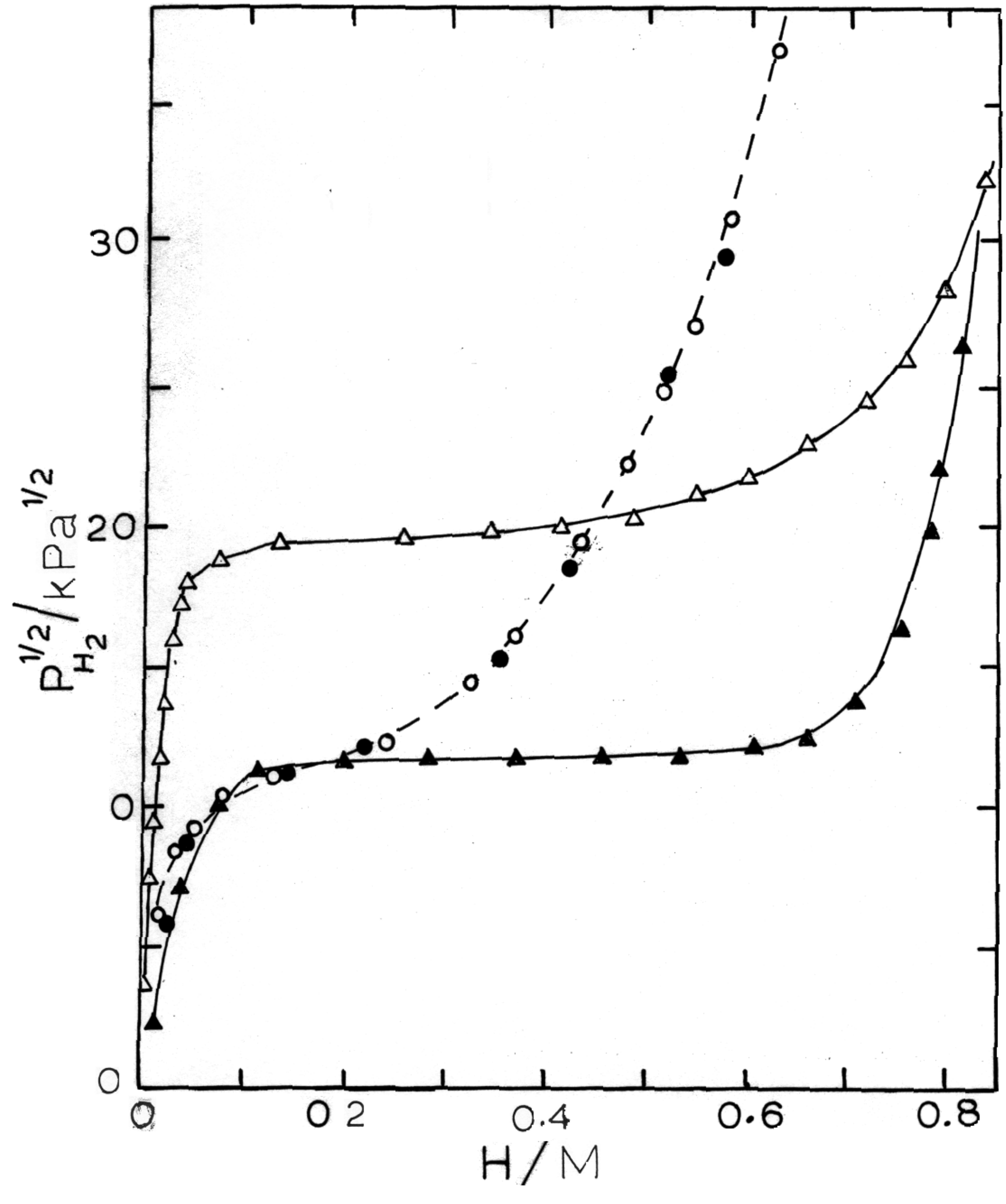

Figure 12.

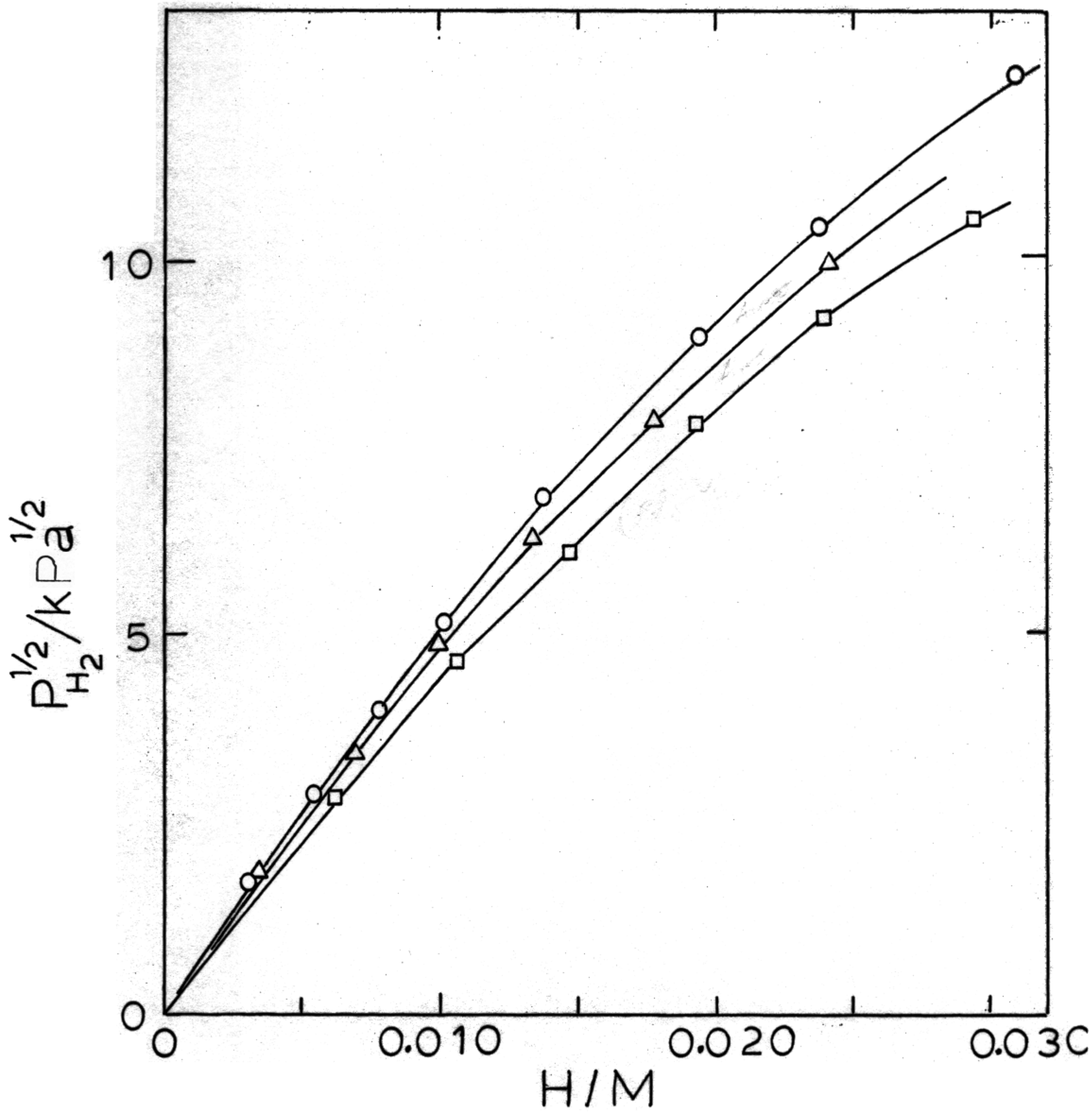

Figure 13.

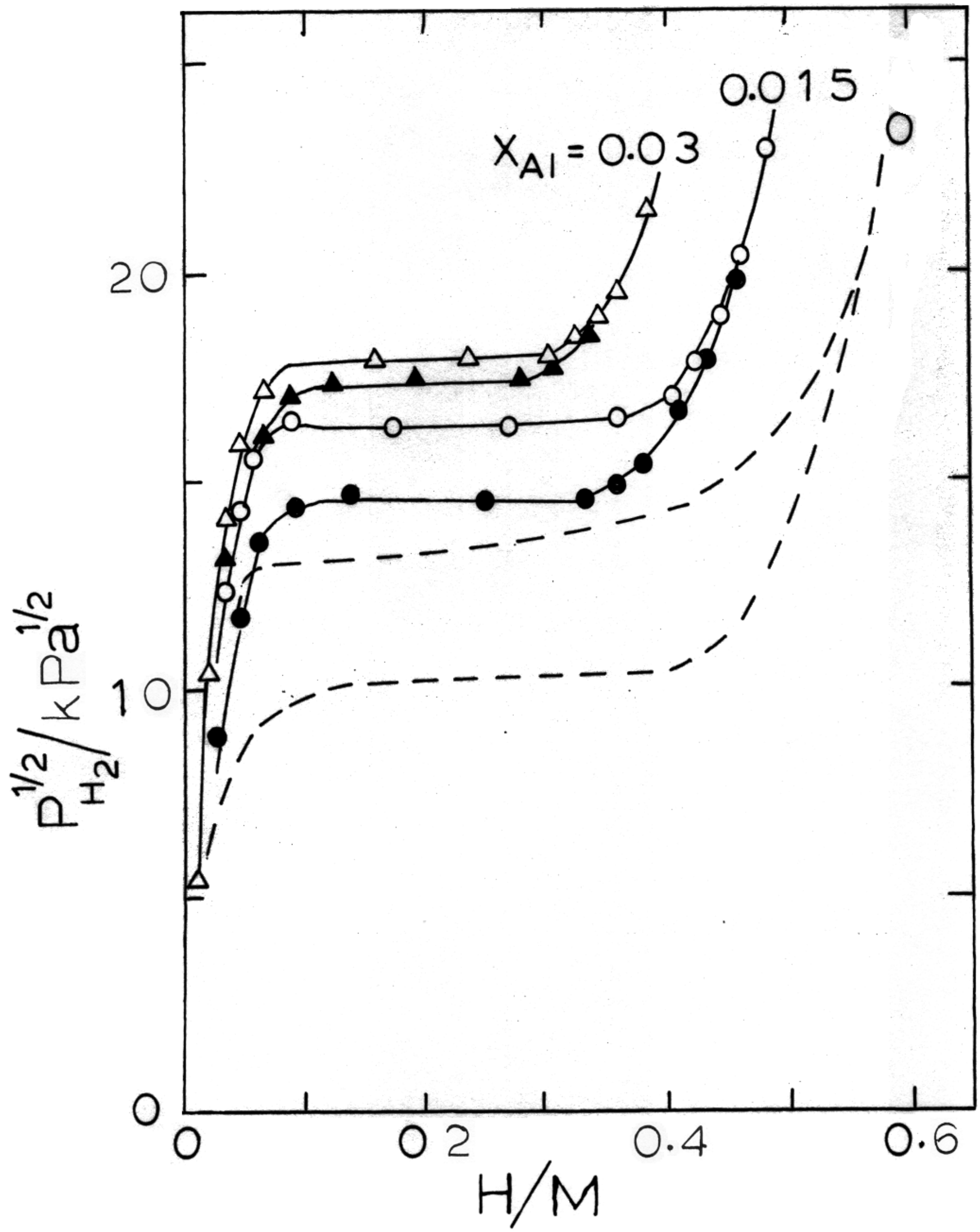

Figure 14.

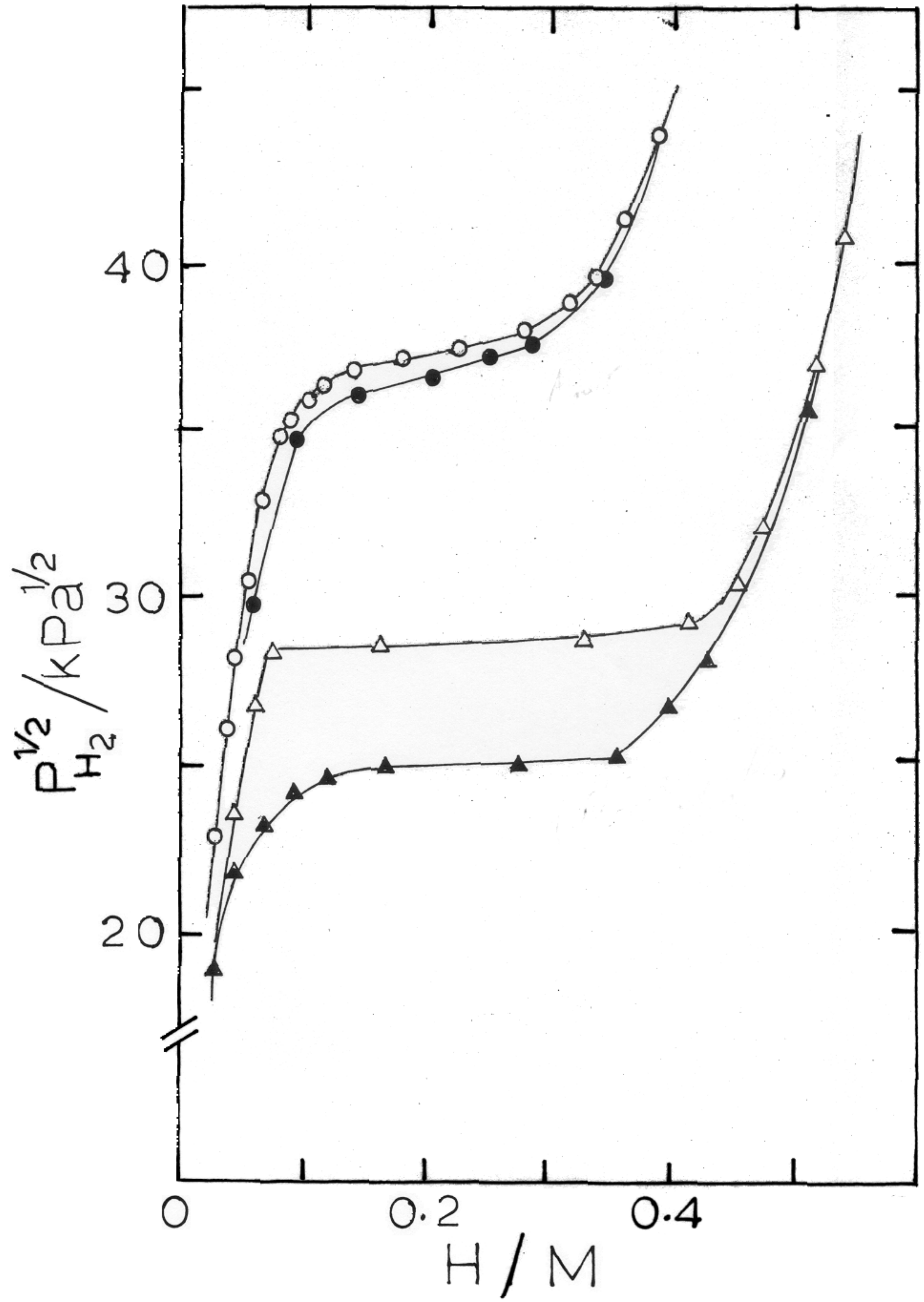

Figure 15.

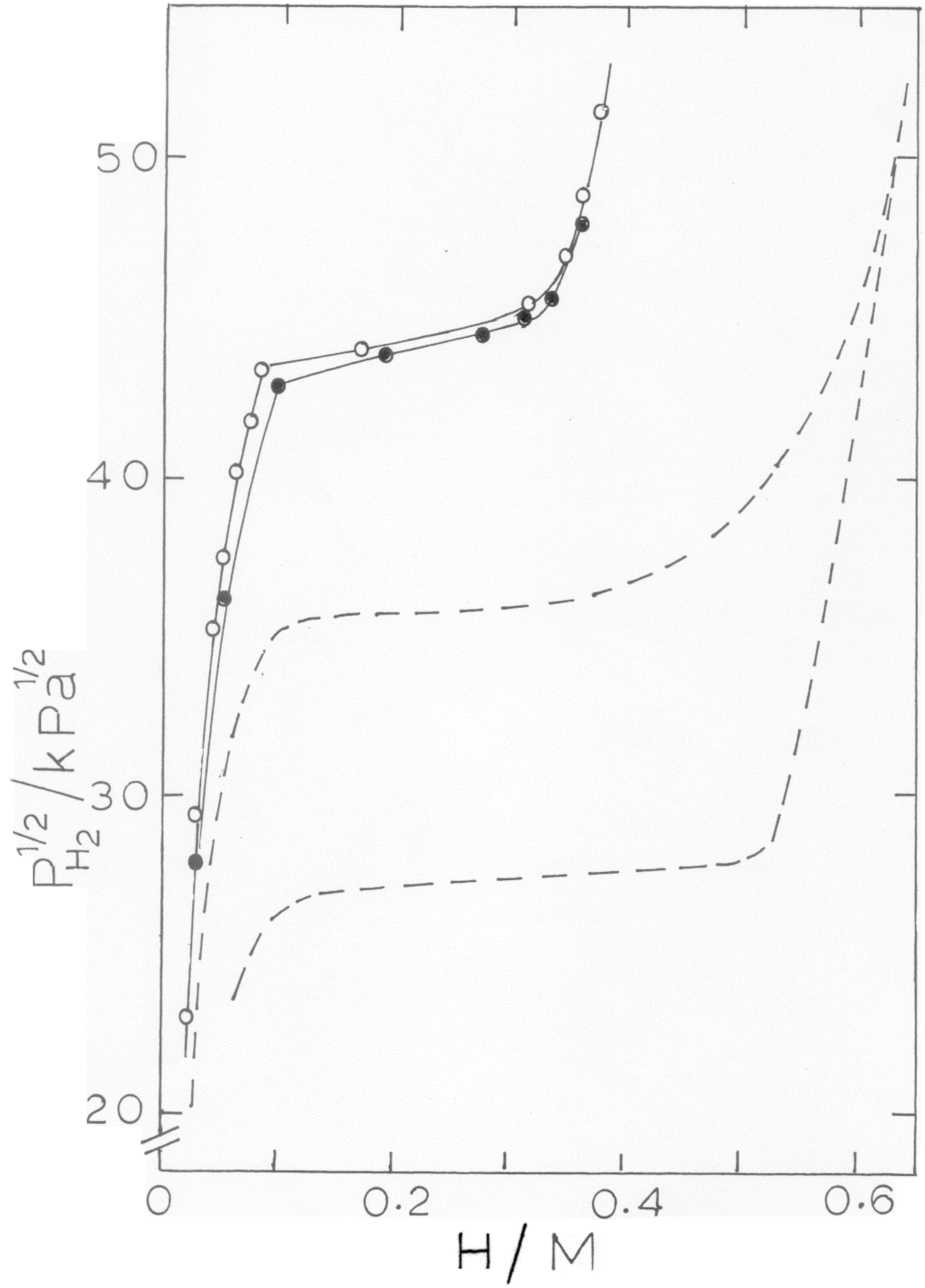

Figure 16.

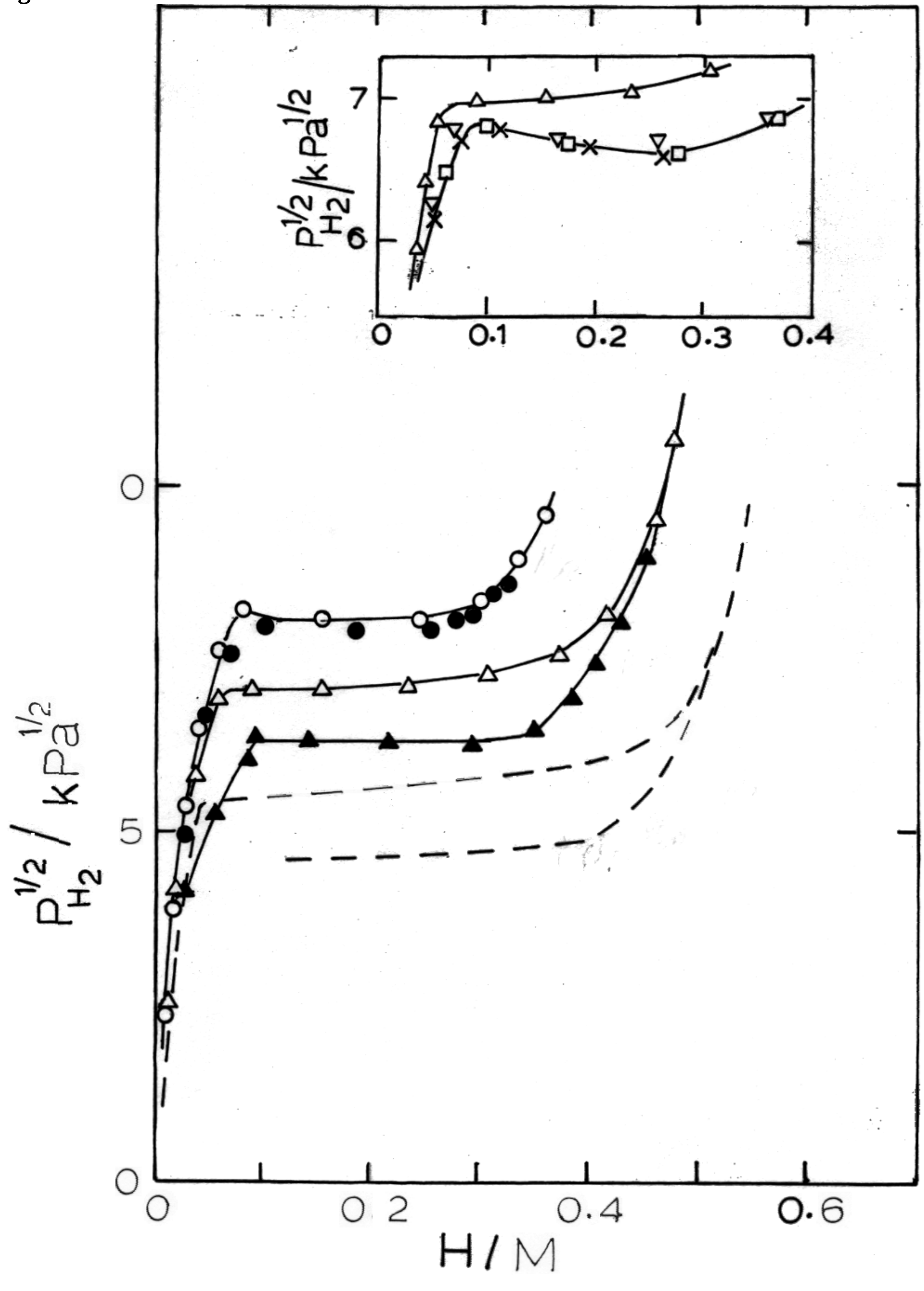

Figure 17.

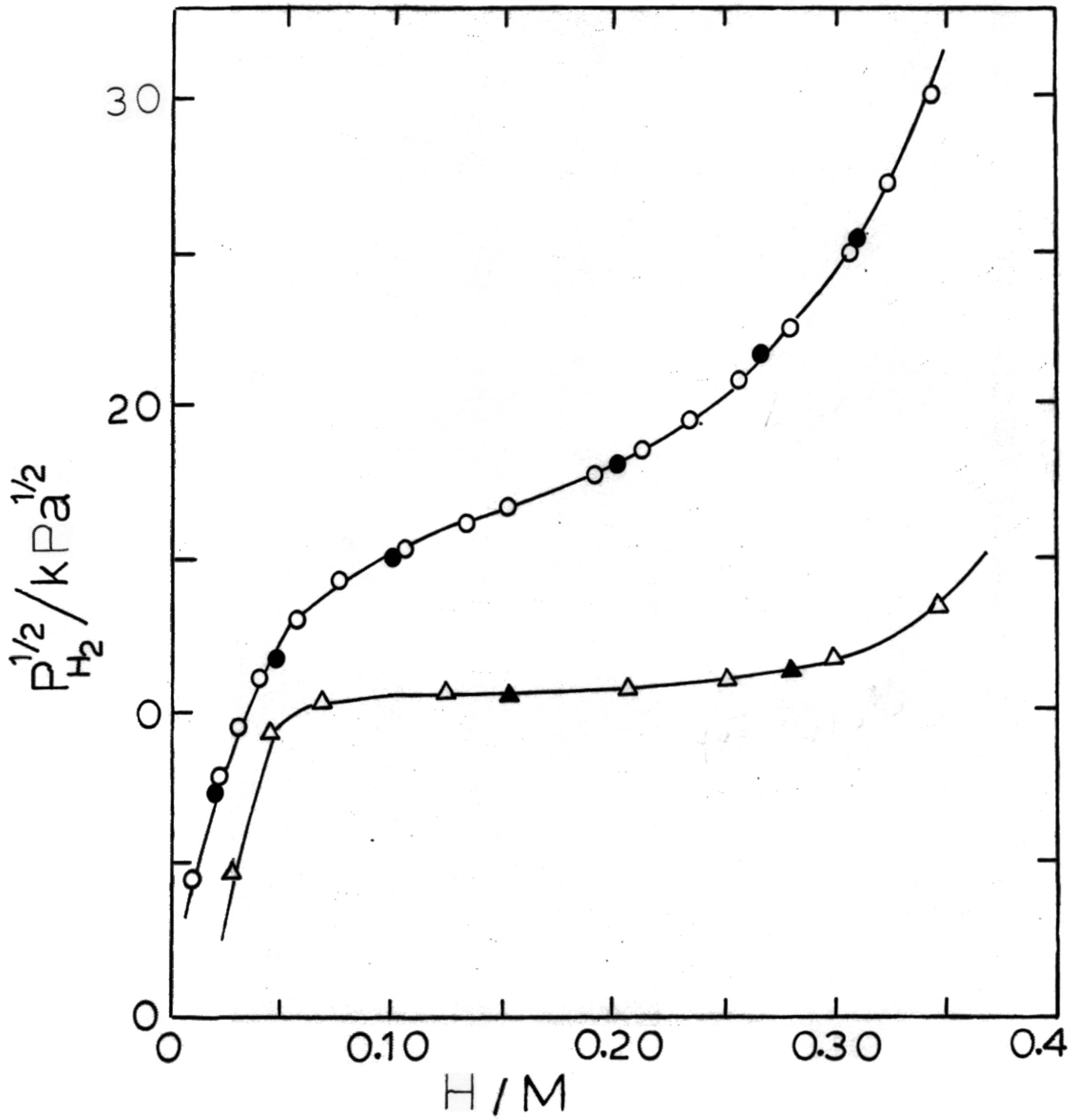

Figure 18.

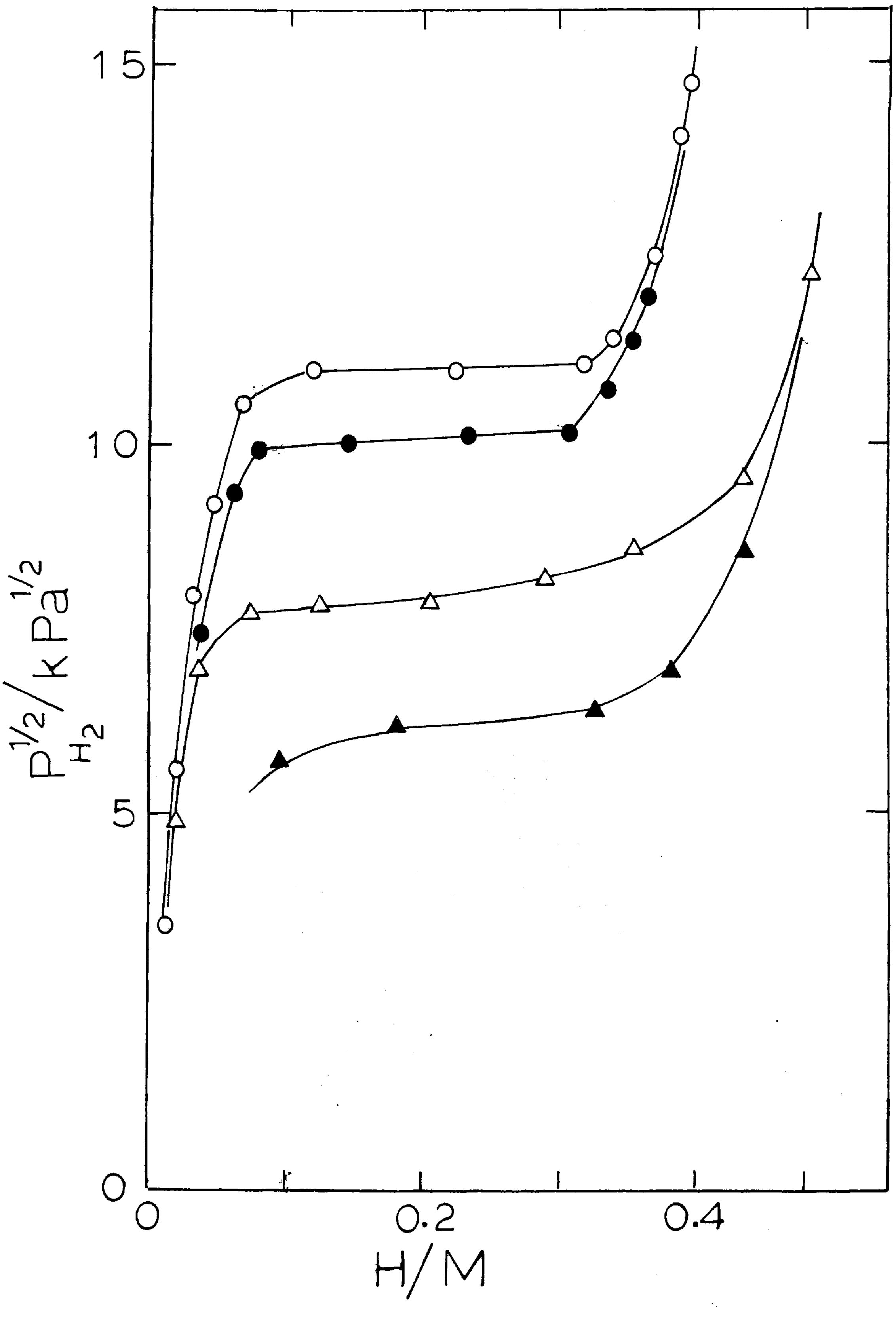

Figure 19.

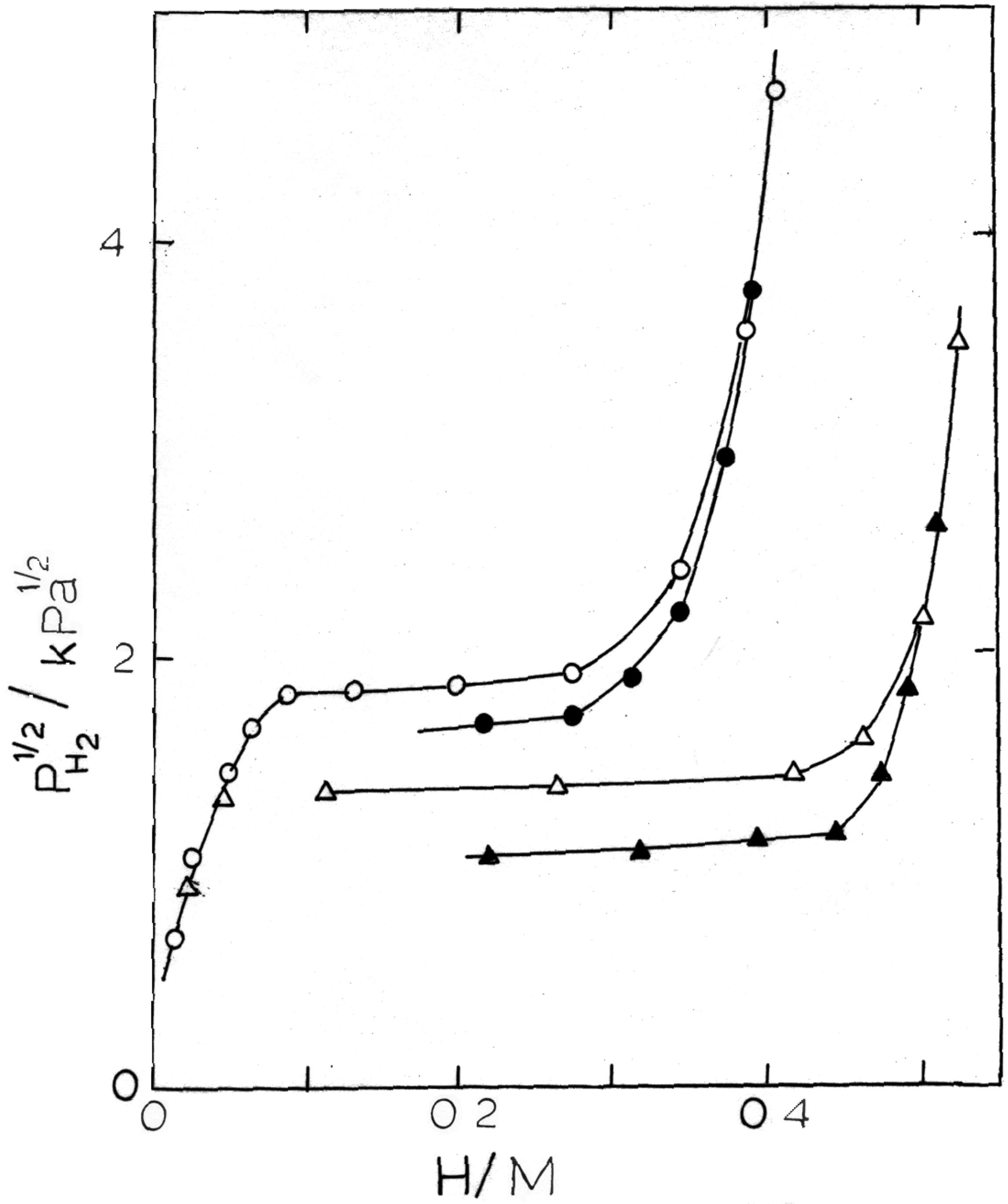

Figure 20.

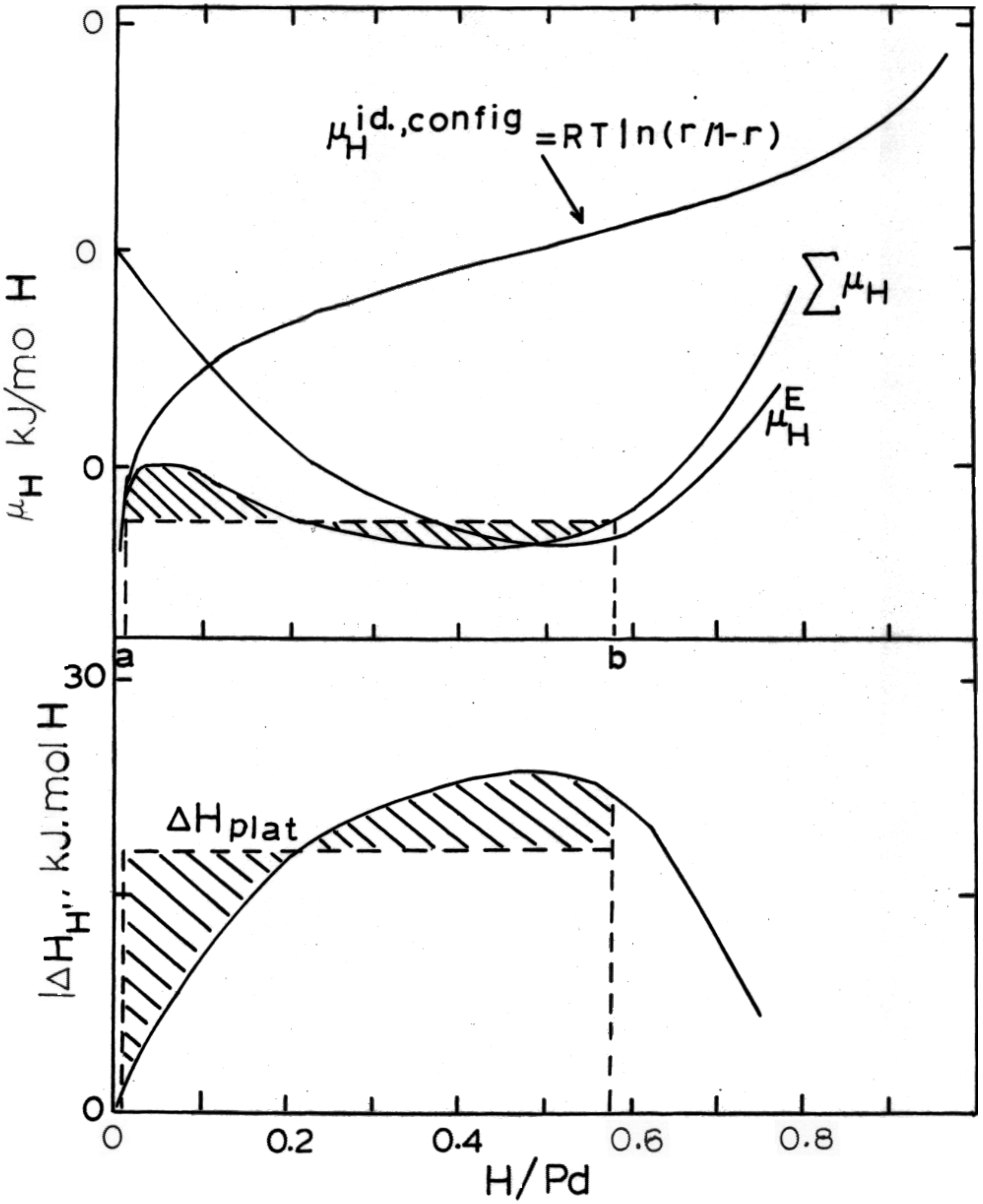
$\mu_H^{id.,config} = RT\ln(r/1-r)$
$\sum\mu_H$
μ_H^E
μ_H kJ/mo H
0
0
0
a
b
30
ΔH_{plat}
$|\Delta H_H|$, kJ.mol H
0
0
0.2
0.4
0.6
0.8
H/Pd

Figure 21.

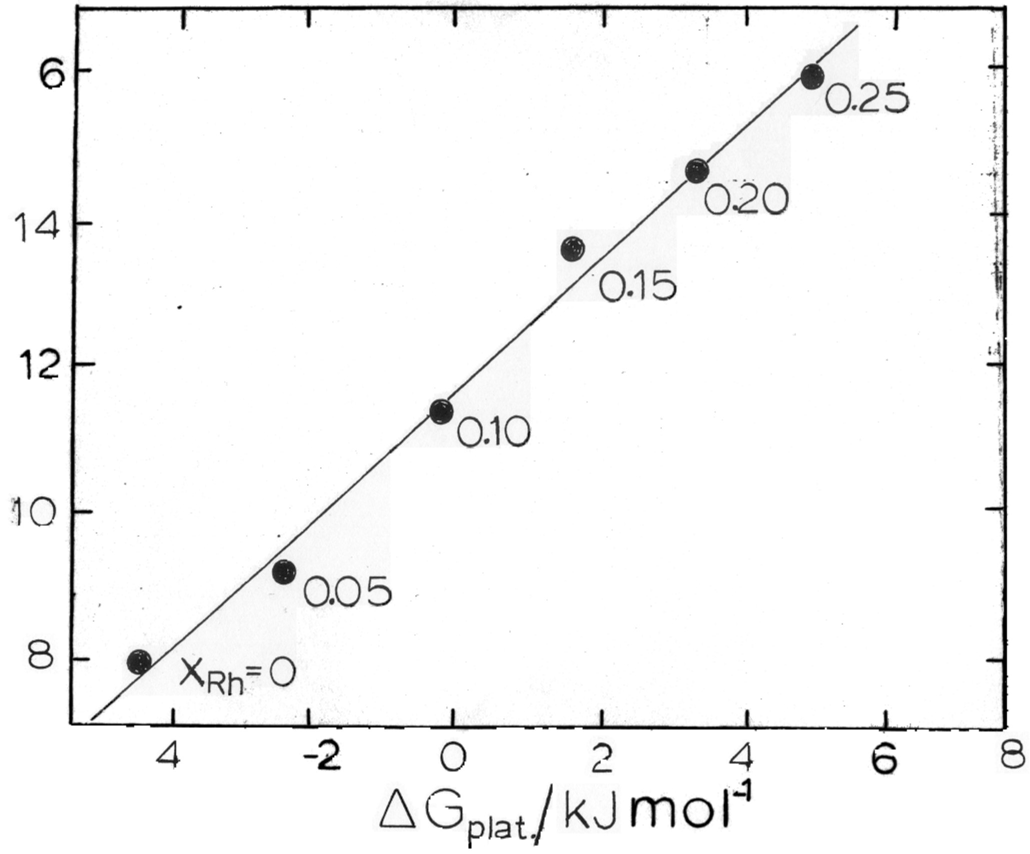
6
14
12
10
8
$\Delta\mu^o_H$/kJ mol^{-1}
4
-2
0
2
4
6
8
$\Delta G_{plat.}$/kJ mol^{-1}
X_{Rh}= 0
0.05
0.10
0.15
0.20
0.25